Dihedral f-tilings of the sphere by triangles and well centered quadrangles

Ana M. d'Azevedo Breda* and Altino F. Santos*

Abstract. In [1] the notion of *well centered spherical quadrangle* (WCSQ) and their properties were described. The study of dihedral f-tilings of the Riemannian sphere S^2 by spherical triangles and WCSQ was initiated in [2], where the classification by spherical triangles and equiangular spherical quadrangles was given. In [3] the classification of dihedral f-tilings by spherical triangles and spherical quadrangles of lozenge type was done. Here we complete the classification of all dihedral f-tilings of S^2 by triangles and well centered quadrangles, presenting the study of dihedral f-tilings by triangles and WCSQ with distinct pairs of congruent opposite angles and with distinct pairs of congruent opposite sides, Figure 80.

1. Introduction

Let us consider the Riemannian sphere S^2. A spherical moon L is said *well centered* if its vertices belong to the great circle $S^2 \cap \{(x, y, z) \in \mathbf{R}^3 \mid x = 0\}$ and the semi-great circle bisecting L contains the point $(1, 0, 0)$. By a *well centered spherical quadrangle* (WCSQ) we mean a spherical quadrangle which is the intersection of two well centered spherical moons with distinct vertices. In [1] it was established that any spherical quadrangle with congruent opposite internal angles is congruent to a WCSQ.

By a *dihedral f-tiling* of the sphere S^2 whose prototiles are a WCSQ Q and a spherical triangle T we mean a polygonal subdivision τ of S^2 such that each *cell* of τ is isometric either to Q or T and all vertices of τ satisfy the *angle-folding relation*.

F-tilings are intrinsically related to the theory of isometric foldings of Riemannian manifolds. See [8] for the foundations of this subject.

Isometric foldings are locally isometries which send piecewise geodesic segments into piecewise geodesic segments of the same length. These maps are

continuous but not necessarily differentiable. The points where they fail to be differentiable are called *singular points*. For surfaces, the singularity set gives rise to a *two-coloured graph* whose vertices fulfill the angle-folding relation, i.e., each vertex is of even valency and the sum of alternating angles is π. For a topological view of this theory see [9].

In [7], Lawrence and Spingarn show that the angle-folding relation is generalized for isometric foldings of the euclidian space $\mathbf{R}^d$. Farran et al. [6] present a study which involves a partition of a surface into polygons.

The complete classification of monohedral tilings of the sphere by triangles (which obviously includes the monohedral triangular f-tilings [4]) was made clear by Yukako Ueno and Yoshio Agaoka [11]. This classification was partially done by D. Sommerville [10], and an outline of the proof was provided by H. Davies [5]. Some examples of spherical tilings by congruent quadrangles are given by Yukako Ueno and Yoshio Agaoka in [12].

Here we discuss dihedral f-tilings by spherical triangles and spherical quadrangles with distinct pairs of congruent opposite internal angles and distinct pairs of congruent opposite sides, completing the classification of dihedral f-tilings by triangles and well centered quadrangles.

Two dihedral f-tilings of S^2, τ_1 and τ_2, are isomorphic iff there is an isometry ψ of S^2 such that $\psi(\tau_1) = \tau_2$. By "unique f-tiling" we mean unique up to an isomorphism. We shall denote by $\Omega(Q, T)$ the set of all dihedral f-tilings of S^2 up to an isomorphism whose prototiles are Q and T.

In [2] it was established that if $\tau \in \Omega(Q, T)$, then τ has vertices of valency four and $\pi < \beta + \gamma + \delta < \frac{3\pi}{2}$ and $\alpha_1 + \alpha_2 > \pi$, where β, γ and δ are the internal angles of T and α_1 and α_2 are the pairs of opposite internal angles of Q.

We shall describe the set $\Omega(Q, T)$, by considering different cases separately depending on the nature of Q and T. If T is an equilateral spherical triangle, then $\Omega(Q, T) = \varnothing$ [3].

In order to get any dihedral f-tilings of $\Omega(Q, T)$, we find it useful to start by considering one of its *planar representation* (PR), beginning with a common vertex to a spherical quadrangle and a spherical triangle in adjacent positions.

We shall denote by WCSQ* a WCSQ with distinct pairs of congruent opposite internal angles and with distinct pairs of congruent opposite sides.

For convenience we label any dihedral f-tiling $\tau \in \Omega(Q, T)$ according to the following procedures:

1. Label 1 the tiles by which we begin the planar representation of the dihedral f-tiling τ;

2. Label a tile j, if the knowledge of the PR of τ by polygons labelled $(1, 2, \ldots, j-1)$ leads, in a unique way, to the extended planar representation $(1, 2, \ldots, j)$.

2. Dihedral f-tilings by isosceles spherical triangles and WCSQ*

Through this section Q and T denote, respectively, a spherical quadrangle and a spherical triangle; Q has, in cyclic order, angle measure $(\alpha_1, \alpha_2, \alpha_1, \alpha_2)$ with $\alpha_1 > \alpha_2$ and distinct pairs of congruent opposite sides and T is an isosceles triangle with internal angles β, γ, γ ($\beta \neq \gamma$). It follows straightaway that $\alpha_1 + \alpha_2 > \pi$ $\left(\alpha_1 > \frac{\pi}{2}\right)$ and $2\gamma + \beta > \pi$.

Any element of $\Omega(Q, T)$ has at least two cells congruent, respectively, to Q and T, such that they are in adjacent positions in one of the situations illustrated in Figure 1.
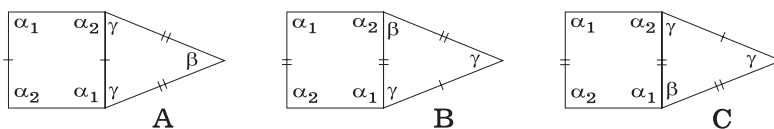

Fig. 1. Distinct cases of adjacency.

PROPOSITION 2.1. *If there are two cells congruent, respectively, to Q and T, such that they are in adjacent positions as presented in Figure 1-A, then $\Omega(Q, T)$ is the empty set.*

PROOF. Suppose that Q and T are in adjacent positions as illustrated in Figure 1-A. Let us consider a vertex surrounded by adjacent angles α_1 and γ. With the labelling of Figure 2-I, $\theta = \beta$ or $\theta = \gamma$, since $\alpha_1 + \alpha_2 > \pi$, $\alpha_1 > \alpha_2$.
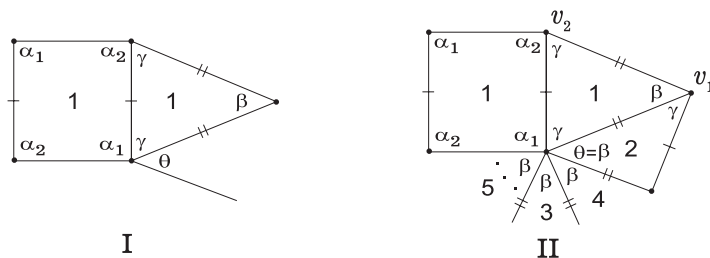

Fig. 2. Planar representations.

If $\alpha_1 + k\beta + l\gamma = \pi$, then $k = 0$ or $l = 0$. This fact easily follows from the conditions $\beta + 2\gamma > \pi$ and $\alpha_1 > \frac{\pi}{2}$.

Suppose firstly that $\theta = \beta$. Then in order to have the angle-folding relation fulfilled, it must be $\alpha_1 + k\beta = \pi = \gamma + k\beta$ for some $k \geq 1$ (Figure 2-II).

And so $\gamma = \alpha_1$. Now, there is no way to obey the angle-folding relation at vertices v_1 and v_2 simultaneously.

Suppose now that $\theta = \gamma$. If $\alpha_1 + \gamma < \pi$, then $\alpha_1 + k\gamma = \pi$ for some $k \geq 2$ (Figure 3-I). It follows that $\gamma < \frac{\pi}{4}$, and so $\beta > \frac{\pi}{2}$, since $\beta + 2\gamma > \pi$. Consequently tile 4 is a triangle and it must be $\beta + \gamma = \pi$. On the other hand, according to the refereed Figure one gets $\beta + \alpha_2 > \beta + \gamma = \pi$, which is an absurd.
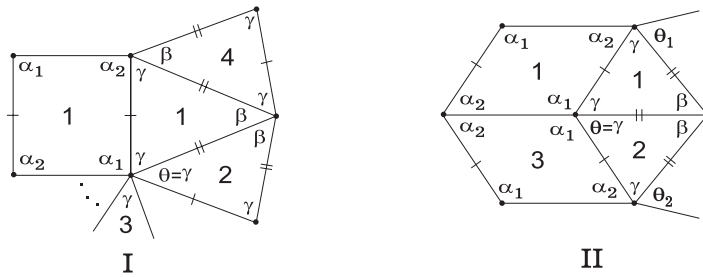

Fig. 3. Planar representations.

If $\alpha_1 + \gamma = \pi$, then $\alpha_1 > \alpha_2 > \gamma$ (Figure 3-II). With the labelling of this Figure one gets

$$\theta_1 = \alpha_2 \qquad \text{or} \qquad \theta_1 = \beta \qquad \text{or} \qquad \theta_1 = \gamma.$$

i) If $\theta_1 = \alpha_2$, then $\alpha_1 + t\beta = \pi$ for some $t \geq 2$. See Figure 4 below. Now, $\beta < \gamma < \alpha_2 < \alpha_1$ and consequently $\alpha_2 + \theta_2 = \alpha_2 + \gamma < \pi < \alpha_2 + \gamma + \rho$ for any $\rho \in \{\alpha_1, \alpha_2, \gamma, \beta\}$, which is not possible.

Fig. 4. Planar representation.

ii) Suppose now that $\theta_1 = \beta$. If $\gamma > \beta$, then we have $\alpha_2 + \beta < \alpha_1 + \gamma = \pi$. But since $\alpha_2 + \beta + \gamma > \beta + 2\gamma > \pi$, the alternated angle sum of this vertex is $\alpha_2 + k\beta = \pi$ ($k \geq 2$). Concerning the remaining alternated angle sum, it is of the form $\gamma + k\beta = \pi$. In fact it contains at least three angles, and if it contains

another γ, then by adding the least angle β, it exceeds π since $2\gamma + \beta > \pi$. And so the remaining alternated angle sum must consist of one γ and k β's. Now, it follows that $\alpha_2 + k\beta = \gamma + k\beta = \pi$, and so $\alpha_2 = \gamma$, which is impossible.

If $\gamma < \beta$, then we have necessarily $\alpha_2 + \beta = \pi$ (observe that $\alpha_2 + \beta + \gamma > \beta + 2\gamma > \pi$ and γ is the least angle). As the quadrangle has distinct pairs of opposite sides, the remaining alternated angle sum (which contains γ) must be $\gamma + \beta = \pi$, leading us to the contradiction $\alpha_2 = \gamma$.

iii) Suppose finally that $\theta_1 = \gamma$. If $\beta < \gamma$, then $\alpha_2 + \theta_1 = \pi$ and so $\alpha_2 = \alpha_1$, which is impossible. And so $\beta > \gamma$. Since an alternated angle sum contains 2β and since $2\beta + \gamma > \pi$, we have $2\beta = \pi$, i.e., $\beta = \frac{\pi}{2}$, and the PR illustrated in Figure 3-II is extended as follows (Figure 5). (Observe that if $\alpha_2 \geq \frac{\pi}{2}$, then $\alpha_2 + \theta_1 = \alpha_2 + \gamma < \pi < \alpha_2 + \gamma + \rho$ for any $\rho \in \{\alpha_1, \alpha_2, \gamma, \beta\}$, which is not possible.)
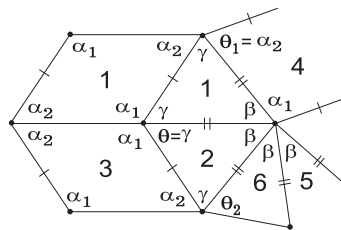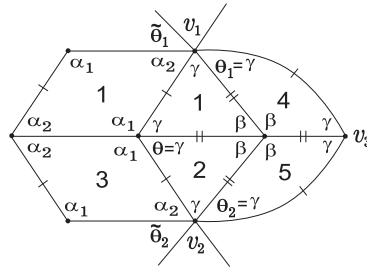

Fig. 5. Planar representation.

Under the above conditions one gets

$$\frac{\pi}{4} < \gamma < \alpha_2 < \frac{\pi}{2} = \beta < \alpha_1. \tag{2.1}$$

One can easily verify that the alternated angle sum containing α_2 and γ (vertex v_1) must be of the form $2\alpha_2 + \gamma$ or $\alpha_2 + 2\gamma$, by using the condition (2.1). Since v_1 has valency six, the remaining alternated angle sum is also exclusively surrounded by angles α_2 and γ.

Taking in account the length sides of T and Q, we may also conclude that $\tilde{\theta}_1 \neq \gamma$ (otherwise, a vertex surrounded by angles β and α_1 takes place. On account of the condition (2.1) the alternated angle sum containing the angle α_1 must be $\alpha_1 + \gamma = \pi$, and the valency of this vertex is four. Then by considering the condition (2.1) and the length sides of T and Q, we can easily arrive at a contradiction). Consequently $\tilde{\theta}_1 = \alpha_2$ and similarly $\tilde{\theta}_2 = \alpha_2$.

Now around the vertex v_1 (and v_2) one has either $\alpha_2 + 2\gamma = \pi$ or $\gamma + 2\alpha_2 = \pi$ ($\alpha_2 > \gamma$). In the first case, by (2.1), vertex v_3 is of the same type

as v_1 and v_2 and then it is easy to verify that we have no way to avoid another vertex surrounded by $(\alpha_1, \beta, \beta, \ldots)$ that cannot be allowed. The second case is illustrated in Figure 6.
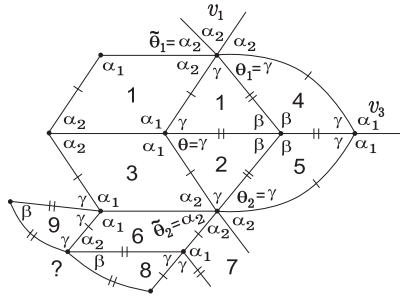

Fig. 6. Planar representation.

Once more, by considering the condition (2.1) and the length sides of the prototiles, we have no way to fulfill the angle-folding relation. And so $\Omega(Q, T)$ is the empty set.   □

Proposition 2.2. *Let Q and T be a spherical quadrangle and a spherical triangle, respectively, such that they are in adjacent positions as illustrated in Figure 1-B. Then, $\Omega(Q, T) \neq \varnothing$ iff $\alpha_1 + \gamma = \pi$, $\alpha_2 + \beta = \pi$ and $\gamma = \frac{\pi}{k}$ for some $k \geq 3$. In this situation for each $k \geq 3$ and $\alpha_2 \in \left]\frac{\pi}{k}, \frac{2\pi}{k}\right[\backslash \{\alpha_2^k\}$ where $\alpha_2^k = \arccos\left(2 \cos \frac{\pi}{k} - 1\right)$, there is a unique dihedral f-tiling denoted by $\mathscr{R}_{\alpha_2}^k$. A planar representation of $\mathscr{R}_{\alpha_2}^k$ is illustrated in Figure 9. 3D representations for $k = 3$ and $k = 4$ are given in Figure 10.*

Proof. Suppose that Q and T are in adjacent positions as illustrated below (or Figure 1-B). Consider also that this PR is contained in a complete PR of any element of $\Omega(Q, T)$. With the labelling used in Figure 7, we have $\theta \neq \alpha_1$ and $\theta \neq \alpha_2$, and taking in account the length sides of Q and T, we must have $\theta = \gamma$. Now, $\alpha_1 + \gamma = \pi$ or $\alpha_1 + \gamma < \pi$.
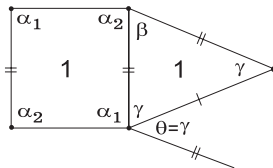

Fig. 7. Planar representation.

i) Suppose that $\alpha_1 + \gamma = \pi$. Then the initial PR is extended to the one illustrated in Figure 8-I.

If $\beta < \gamma$, then $\alpha_1 > \alpha_2 > \gamma > \beta$. Consider an alternated angle sum containing α_2 at the vertex v_1. We show that the angle adjacent to β is also β. Clearly this angle cannot be α_1. If it is γ, then $\gamma + \alpha_2 < \gamma + \alpha_1 = \pi$ and by adding the least angle β, it exceeds π. And hence it is not γ. If it is α_2, then we have $2\alpha_2 \leq \pi$. If $2\alpha_2 < \pi$, then we have a contradiction by the same reason as above. Hence we have $2\alpha_2 = \pi$, and the valency of v_1 is four. But this is impossible because $\pi = \alpha_1 + \gamma > \alpha_1 + \beta$. Therefore this angle is β. Then an alternated angle sum at the vertex v_2 contains 2γ, and we have $2\gamma \leq \pi$. If $2\gamma < \pi$, then by adding the least angle β, we have $\beta + 2\gamma > \pi$, which is a contradiction. Hence we have $2\gamma = \pi$, but this is also a contradiction because we have $\alpha_1 + \gamma = \pi$ and $\alpha_1 \neq \gamma$.

If $\beta > \gamma$, then $\alpha_1 > \alpha_2 > \gamma$ and $\alpha_1 \geq \beta > \gamma$ (observe that if $\beta > \alpha_1$, then $\beta + \rho > \pi = \alpha_1 + \gamma$ for any $\rho \in \{\alpha_1, \alpha_2, \gamma, \beta\}$, which is not allowed). As Q has distinct pairs of opposite sides, we have only one way to signalize the length sides of tile 4 (Figure 8-II).
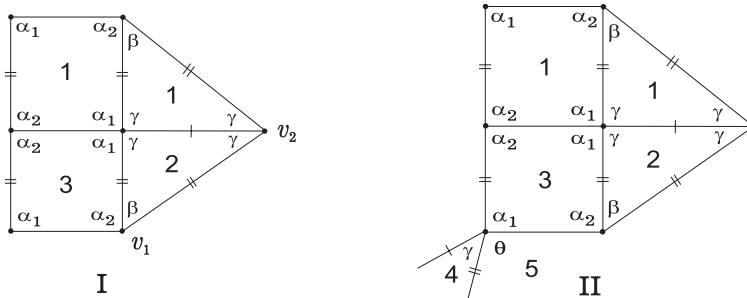
Fig. 8. Planar representations.

With the labelling used in this Figure if $\theta = \gamma$, then the angle of tile 5 adjacent to α_2 must be γ, and we have $\gamma + \beta \leq \pi$. If $\gamma + \beta < \pi$, then by adding the least angle, it exceeds π. And hence $\gamma + \beta = \pi$. By considering the length sides of the prototiles, the remaining alternated angle sum must be $\alpha_2 + \beta = \pi$. Consequently, $\alpha_2 = \gamma$, which is not possible. And so $\theta = \alpha_1$. This information permit us to conclude that $\alpha_2 + \beta = \pi$ and $\gamma = \frac{\pi}{k}$ for some $k \geq 3$.

An extended PR is illustrated in Figure 9, where $\alpha_1 + \gamma = \pi$, $\alpha_2 + \beta = \pi$ and $\gamma = \frac{\pi}{k}$ for some $k \geq 3$.

Let $A(T)$ denote the area of T. Then

$$0 < A(T) < \frac{\pi}{k} \quad \text{i.e.} \quad \frac{\pi}{k} < \alpha_2 < \frac{2\pi}{k}, \quad k \geq 3 \quad \left(\pi - \frac{2\pi}{k} < \beta < \pi - \frac{\pi}{k}\right).$$

Fig. 9. Planar representations.
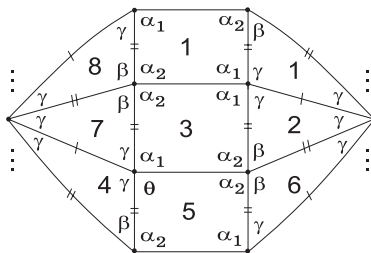
Note that for any $\beta \in {]}\pi - \frac{2\pi}{k}, \pi - \frac{\pi}{k}[$ and any $k \geq 3$, we have $\beta > \gamma = \frac{\pi}{k}$, and if $k \geq 4$, then $\beta > \frac{\pi}{2} > \alpha_2$.

If $\alpha_2 = \frac{\pi}{k}$ $(\beta = \pi - \frac{\pi}{k})$, then one gets a monohedral f-tiling with prototile T of angles $\pi - \frac{\pi}{k}$, $\frac{\pi}{k}$ and $\frac{\pi}{k}$ $(k \geq 3)$ obtained in [4] and [11].

In [3] it was established that if $\alpha_2 = \arccos(2\cos\frac{\pi}{k} - 1) = \alpha_2^k$, then Q has all congruent sides, and so α_2^k must be excluded. In fact, Q has all congruent sides iff

$$\frac{\cos\gamma(1 + \cos\beta)}{\sin\gamma\sin\beta} = \frac{\cos\frac{\alpha_1}{2}(1 + \cos\alpha_2)}{\sin\frac{\alpha_1}{2}\sin\alpha_2}$$

i.e.,

$$\frac{\cos\frac{\pi}{k}(1 - \cos\alpha_2)}{\sin\frac{\pi}{k}\sin\alpha_2} = \frac{\sin\frac{\pi}{2k}(1 + \cos\alpha_2)}{\cos\frac{\pi}{2k}\sin\alpha_2}.$$

And so

$$\tan\frac{\pi}{k} \cdot \tan\frac{\pi}{2k} = \tan^2\frac{\alpha_2}{2}. \tag{2.2}$$

The unique solution of (2.2) in the interval $]\frac{\pi}{k}, \frac{\pi}{2k}[$ is α_2^k, as seen in [3]. In Figure 10 3D representations for $k = 3$ and $k = 4$ are illustrated.

ii) If $\alpha_1 + \gamma < \pi$, then in order to fulfill the angle-folding relation we must have $\alpha_1 + k\gamma = \pi$ for some $k \geq 2$. Consequently $\beta > \alpha_1 > \alpha_2 > \gamma$ and so there is no way to verify the angle-folding relation around any vertex surrounded by α_2 and β in adjacent positions (observe that there is at least one vertex in such a condition). □

PROPOSITION 2.3. *If there are two cells congruent to Q and T, respectively, such that they are in adjacent positions as in Figure 1-C, then $\Omega(Q, T) \neq \varnothing$ iff $\gamma = \frac{\pi}{2}$, $\alpha_2 + \gamma = \pi$ and $\alpha_1 + k\beta = \pi$ for some $k \geq 1$. In this situation for each $k \geq 1$ and $\beta \in {]}0, \frac{\pi}{2k}[$ there is a unique f-tiling denoted by $\mathcal{D}_\beta^k$. Planar repre-*
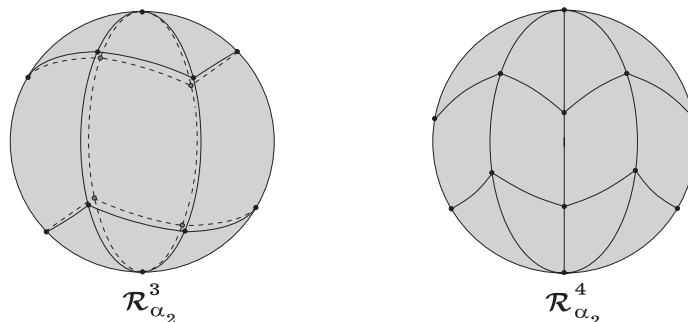
Fig. 10. 3D representations.

sentations for $k = 1$ and $k = 2$ are given in Figure 14. *Also* 3D *representations are given in Figure* 16.

PROOF. We shall discern the following situations:

i) $\gamma \geq \dfrac{\pi}{2}$ and $\alpha_2 + \gamma < \pi$;   ii) $\gamma \geq \dfrac{\pi}{2}$ and $\alpha_2 + \gamma \geq \pi$;   iii) $\gamma < \dfrac{\pi}{2}$.

i) Suppose firstly that $\gamma \geq \frac{\pi}{2}$ and $\alpha_2 + \gamma < \pi$. Let v be a vertex belonging to adjacent tiles, congruent to Q and T, and surrounded by α_1 and β, as shown in Figure 11-I.
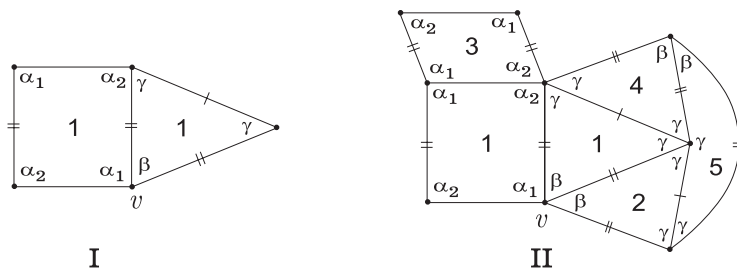
Fig. 11. Planar representations.

As $\alpha_1 > \frac{\pi}{2}$, $\gamma \geq \frac{\pi}{2}$ and $\alpha_1 + \alpha_2 > \pi$, the alternated angle sum containing α_1 at the vertex v is given by $\alpha_1 + k\beta = \pi$ for some $k \geq 1$. On the other hand, as Q has distinct pairs of opposite sides and, as $\alpha_2 < \frac{\pi}{2} \leq \gamma$, tile 3 is completely determined as shown in Figure 11-II. Now, $\alpha_2 + \alpha_1 > \pi$ and $\gamma + \alpha_1 > \pi$ and so the tile 4 is also completely determined (see length sides), leading us to conclude that $\gamma = \frac{\pi}{2}$. Using similar arguments, we may extend this PR to the one that follows (Figure 12). This procedure leads us to a vertex surrounded by

adjacent angles given by $(\gamma, \gamma, \alpha_2, \alpha_2, \gamma, \ldots)$ in cyclic order with $\gamma + \alpha_2 < \pi < \gamma + \alpha_2 + \gamma$, which is an absurd.
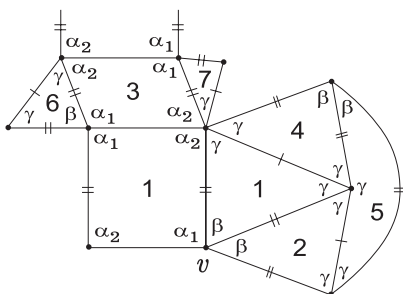
Fig. 12.   Planar representation.

ii) Suppose now that $\gamma \geq \frac{\pi}{2}$ and $\alpha_2 + \gamma \geq \pi$. Similarly to the previous case we must have (Figure 13-I)

$$\alpha_1 + k\beta = \pi, \qquad \text{for some } k \geq 1. \tag{2.3}$$
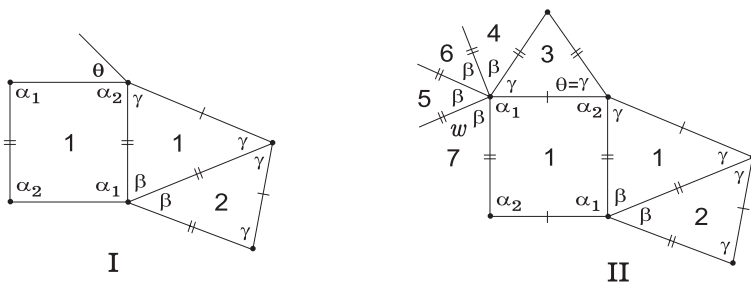
Fig. 13.   Planar representations.

With the labelling of this Figure we may observe that $\theta = \gamma$ or $\theta = \alpha_2$.

If $\theta = \gamma$, then $\gamma = \frac{\pi}{2}$ and the PR is extended as shown in Figure 13-II. One gets a vertex w such that the alternated angle sums around it are of the form $\alpha_1 + k\beta = \pi = \gamma + k\beta$ for some $k \geq 1$. This is a contradiction since $\frac{\pi}{2} = \gamma < \alpha_1$.

If $\theta = \alpha_2$, then it is a straightforward exercise (see 2.3)) to show that for each $k \geq 1$ the PR illustrated in Figure 13-I is extended in a unique way, where the alternated angle sum around vertices satisfy

$$\gamma + \gamma = \pi, \qquad \alpha_2 + \gamma = \pi \qquad \text{and} \qquad \alpha_1 + k\beta = \pi, \quad k \geq 1.$$

Complete *PR's* for the cases $k = 1$ and $k = 2$ are given in Figure 14-I and Figure 14-II, respectively.
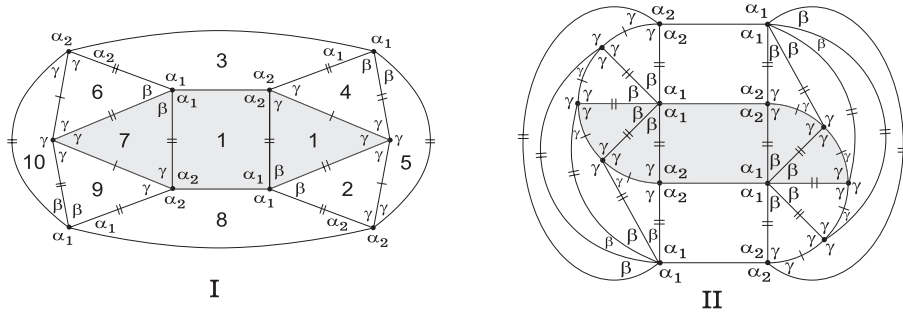
Fig. 14. Planar representations.

Any extended planar representation contains a spherical moon (the dark region) of angle $\gamma = \frac{\pi}{2}$. It is composed of one quadrangle at its center and $2k$ $(k \geq 1)$ triangles.

Let b and c denote the length sides of T opposite to β and γ, respectively. As $\gamma = \frac{\pi}{2}$ and T is an isosceles triangle with angles β, γ, γ, we have $c = \frac{\pi}{2}$ and $b = \beta$ (Figure 15). Now, if $\tilde{c}$ is the side of the quadrangle, which is not common to any side of the triangle, then $\tilde{c} + kb = \tilde{c} + k\beta = \frac{\pi}{2}$. Besides, we may have $0 < k\beta < \frac{\pi}{2}$.
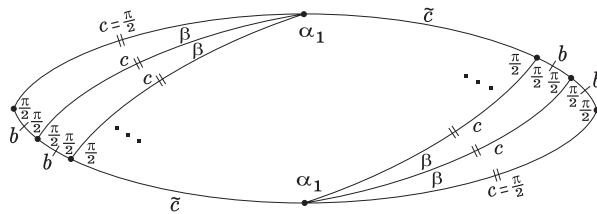
Fig. 15. A tiled spherical moon.

In Figure 16-I and Figure 16-II 3D representations for $k = 1$ and $k = 2$ are illustrated, respectively. They are obtained by reflecting the refereed tiled spherical moon on its edges. We shall denote the correspondent f-tiling by $\mathscr{D}_\beta^k$, $\beta \in \left]0, \frac{\pi}{2k}\right[$, $k \geq 1$. It is composed of 4 quadrangles and $8k$ triangles.

iii) Finally we shall suppose that $\gamma < \frac{\pi}{2}$. Let v be a vertex belonging to adjacent tiles congruent to Q and T and surrounded by β. A planar
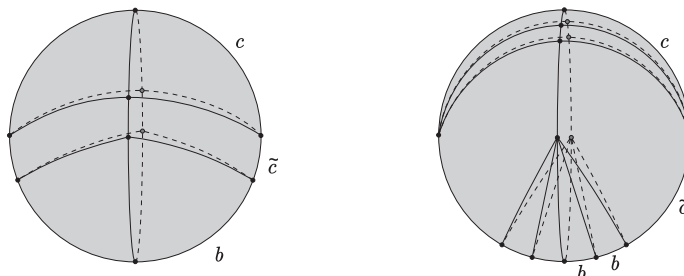
Fig. 16. 3D representations of $\mathscr{D}_\beta^1$ and $\mathscr{D}_\beta^2$.

representation near v is illustrated in Figure 17. Since $\alpha_1 + \alpha_2 > \pi$, we have $\theta \in \{\gamma, \beta\}$, according to the labelling of the refereed Figure.
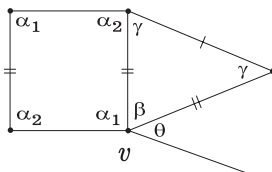
Fig. 17. Planar representation.

If $\theta = \gamma$ and $\alpha_1 + \gamma < \pi$, then we must have $\alpha_1 + k\gamma = \pi$ for some $k \geq 2$. Consequently $\gamma < \frac{\pi}{4}$ and so $\gamma < \alpha_2 < \alpha_1 < \beta$. Now the alternated angle sum containing β at the vertex v cannot be defined, since $\beta + 2\gamma > \pi$. If $\alpha_1 + \gamma = \pi$, then we have no way to set up one fourth tile around v, since Q has distinct pairs of congruent opposite sides.

Suppose then that $\theta = \beta$. If $\alpha_1 + \beta = \pi$ $\left(\beta < \frac{\pi}{2} < \alpha_1\right)$, then the *PR* illustrated in Figure 17 is extended as follows (see Figure 18-I). With
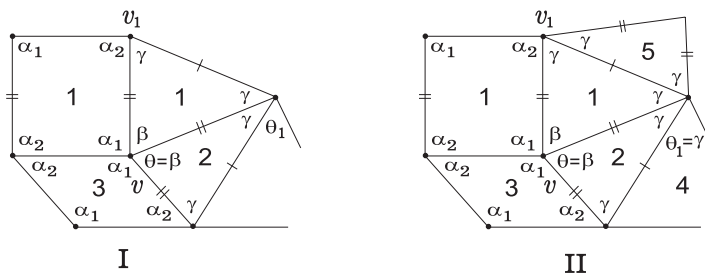
Fig. 18. Planar representations.

the labelling of this Figure, $\theta_1 \in \{\alpha_1, \gamma\}$. If $\theta_1 = \alpha_1$, then $\gamma + \alpha_1 \leq \pi$. But, since $\beta \neq \gamma$, we have $\gamma + \alpha_1 < \pi$. Now, $\gamma + \alpha_1 < \pi < \gamma + \alpha_1 + \rho$ for any $\rho \in \{\alpha_1, \alpha_2, \beta, \gamma\}$. Consequently $\theta_1 = \gamma$. It follows that the alternated angle sum containing θ_1 is $k\gamma = \pi$ for some $k \geq 3$. In fact one has $2\gamma \leq \pi$. But, since $\gamma < \frac{\pi}{2}$, we must have $2\gamma < \pi$. As $\alpha_1 > \alpha_2 > \beta$ (note that, we always have $\alpha_1 + \alpha_2 > \pi$, and here, we also have $\alpha_1 + \beta = \pi$) and $2\gamma + \beta > \pi$, we have $k\gamma = \pi$ $(k \geq 3)$. And hence $\beta > \gamma$ (Figure 18-II). Considering now the alternated angle sum containing α_2 at the vertex v_1, one gets $\alpha_2 + \gamma < \pi < \alpha_2 + \gamma + \rho$ for any $\rho \in \{\alpha_1, \alpha_2, \beta, \gamma\}$ which is a contradiction.

If $\alpha_1 + \beta < \pi$ (therefore $\alpha_1 > \alpha_2 > \beta$), then one gets $(\alpha_1, \beta, \beta, \ldots, \beta, \alpha_1)$ with $\alpha_1 + t\beta = \pi$ $(t \geq 2)$ as the cyclic sequence of angles around v (Figure 19-I). Since $\alpha_1 > \frac{\pi}{2}$, we have $t\beta < \frac{\pi}{2}$, and hence $\beta < \frac{\pi}{4} < \gamma$. According to the labelling of Figure 19-I, one has $\theta_2 \neq \gamma$ (if $\theta_2 = \gamma$, then $\gamma + \gamma < \pi < \gamma + \gamma + \rho$ for any $\rho \in \{\alpha_1, \alpha_2, \beta, \gamma\}$). It follows immediately that $\theta_2 = \alpha_1$ and the previous PR is extended as illustrated in Figure 19-II, where $\alpha_1 + \gamma = \pi$. And so $\alpha_1 > \alpha_2 > \gamma > \beta$. A vertex w enclosed by the cyclic sequence $(\alpha_2, \gamma, \gamma, \ldots)$ with $\alpha_2 + \gamma < \pi < \alpha_2 + \gamma + \beta$ must take place, which is an absurd. $\qquad \square$
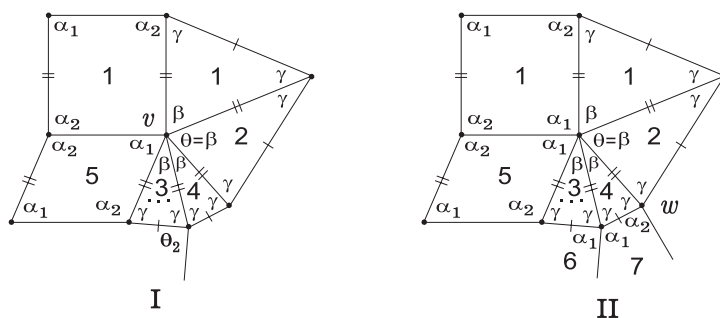
Fig. 19. Planar representations.

REMARK. Considering $k = 2$ in Proposition 2.2 and permuting α_1 with α_2, one gets the f-tilings $\mathscr{D}_\beta^1$, obtained in Proposition 2.3. Thus, attending to the configuration of "$\mathscr{R}^k$", we may define $\mathscr{R}_{\alpha_2}^2$, as being $\mathscr{D}_\beta^1$ $(0 < \beta < \frac{\pi}{2}$ and $\frac{\pi}{2} < \alpha_2 < \pi)$, as long as $\alpha_2 + \beta = \pi$.

3. Dihedral f-tilings by scalene spherical triangles and WCSQ*

Now T stands for a scalene spherical triangle of internal angles β, γ and δ with $\beta > \gamma > \delta$ $(\beta + \gamma + \delta > \pi)$, and Q is a spherical quadrangle with distinct pairs of congruent opposite sides and distinct pairs of congruent opposite angles, α_1 and α_2, such that $\alpha_1 > \alpha_2$. It follows that $\alpha_1 + \alpha_2 > \pi$ and so, $\alpha_1 > \frac{\pi}{2}$.

If $\tau \in \Omega(Q,T)$, then there are necessarily two cells of τ congruent to Q and T, respectively, such that they are in adjacent positions in one of the situations illustrated in Figure 20.
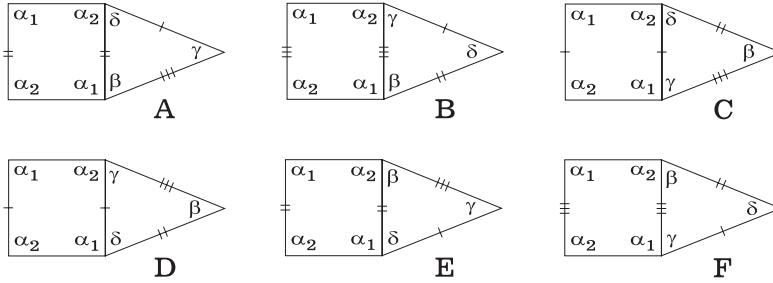
Fig. 20.   Distinct cases of adjacency.

PROPOSITION 3.1.   *If there are two cells congruent to Q and T, respectively, such that they are in adjacent positions as illustrated in Figure* 20-A *or Figure* 20-B *(cases when α_1 and β are in adjacent positions), then $\Omega(Q,T) = \varnothing$.*

PROOF.   A) Suppose firstly that there are two cells in adjacent positions as illustrated in Figure 20-A. Let θ be the angle adjacent to β and opposite to α_1. It follows that $\theta = \beta$ or $\theta = \gamma$.

i)   If $\theta = \beta$, then necessarily $\alpha_1 + \beta = \pi$. In fact if $\alpha_1 + \beta < \pi$ $\left(\alpha_1 > \frac{\pi}{2}\right)$, then $\alpha_1 + \beta + \rho > \beta + \gamma + \delta > \pi$ for any $\rho \in \{\alpha_1, \alpha_2, \beta, \gamma, \delta\}$, which is a contradiction. The *PR* is then extended as illustrated in Figure 21.
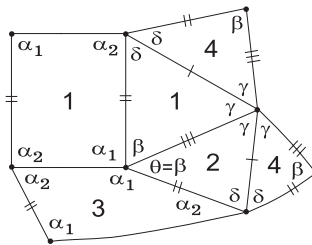
Fig. 21.   Planar representation.

The present relation between angles is $\alpha_1 > \alpha_2 > \beta > \gamma > \delta$, which allows tiles labelled by 4 to be completely determined. One gets a vertex surrounded by at least four γ angles. As $\alpha_1 > \frac{\pi}{2} > \beta$ and $\beta + \gamma + \delta > \pi$, we have $\gamma + \delta > \frac{\pi}{2}$ and $\gamma > \frac{\pi}{4}$. Consequently this vertex is of valency six and surrounded by exclusively angles γ (see length sides), leading to $\gamma = \frac{\pi}{3}$. By the present relation

between angles we must have $\alpha_2 + k\delta = \pi$ for some $k \geq 2$. Now, if the tile 6 was a quadrangle (see Figure 22-I), then one would get at least a vertex surrounded by angles α_2, γ and δ. In fact, with the labelling of this Figure, we have clearly $\varepsilon_1 \neq \alpha_1$ and $\varepsilon_1 \neq \alpha_2$, and if $\varepsilon_1 = \gamma$, then $\alpha_1 + \gamma < \alpha_1 + \beta = \pi < \alpha_1 + \gamma + \rho$ for any $\rho \in \{\alpha_1, \alpha_2, \beta, \gamma, \delta\}$. And so $\varepsilon_1 = \beta$ or $\varepsilon_1 = \delta$. In any case, it comes $\varepsilon_2 = \gamma$, by using the length sides of T and Q. And so a vertex surrounded by the cyclic sequence $(\delta, \delta, \alpha_2, \gamma, \delta, \ldots)$ takes place. Around this vertex an incompatibility between sides can not be avoided. Hence the tile 6 must be a triangle permitting us to adjoin some more cells to get the PR illustrated in Figure 22-II. This procedure gives rise to a vertex surrounded by the cyclic sequence $(\beta, \beta, \beta, \ldots)$, leading us to a contradiction since $2\beta < \pi < 2\beta + \rho$ for any $\rho \in \{\alpha_1, \alpha_2, \beta, \gamma, \delta\}$.
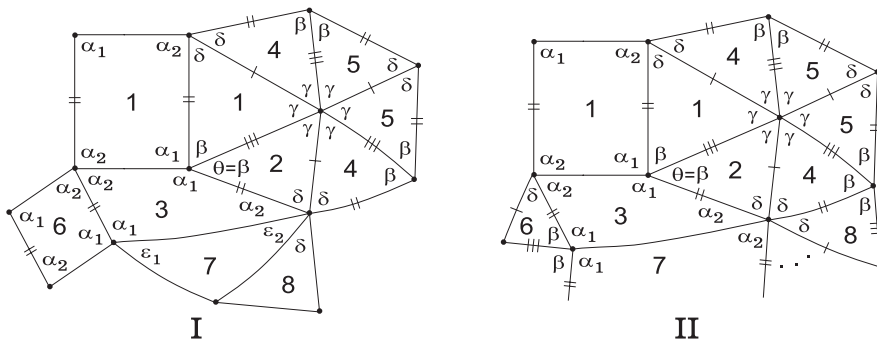
Fig. 22. Planar representations.

ii) Suppose now that $\theta = \gamma$. Taking in account the length sides of Q and T, if $\alpha_1 + \gamma = \pi$, then we have necessarily $\alpha_1 + \gamma = \pi = \beta + \gamma$ (see Figure 23-I). One has a vertex surrounded by α_2 and β in adjacent positions. Analyzing the length sides of the prototiles we must have $\beta + k\delta = \pi$ for some $k \geq 2$. The alternated angle sum containing α_2 has to be $\alpha_2 + k\delta = \pi$. Therefore $\alpha_2 = \beta = \alpha_1$, which is a contradiction.

If $\theta = \gamma$ and $\alpha_1 + \gamma < \pi$ (Figure 23-II), then $\alpha_1 + \gamma + \delta \leq \pi$, since δ is the least angle that we may add to complete such alternated angle sum. As $\beta + \gamma + \delta > \pi$, $\beta > \alpha_1$, and we also have $\alpha_1 > \alpha_2 > \gamma > \delta$. Since the valency of this vertex is greater that four, the alternated angle sum containing β must be $\beta + t\delta = \pi$ for some $t \geq 2$. On the other hand Q has distinct pairs of opposite sides, leading to an incompatibility between sides.

B) Suppose now that there are two cells in adjacent positions as illustrated in Figure 20-B. Let θ be the angle adjacent to β and opposite to α_1. It follows that $\theta = \beta$ or $\theta = \delta$.
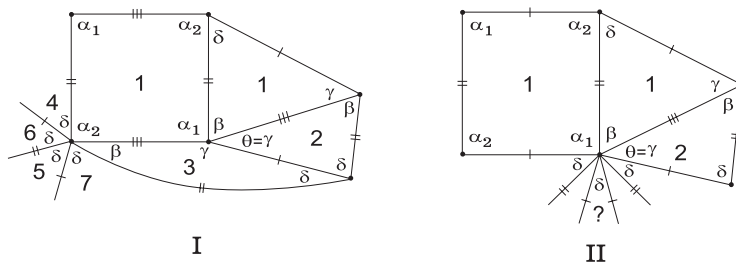
Fig. 23. Planar representations.

i) If $\theta = \beta$, then as before $\alpha_1 + \beta = \pi$. And so $\alpha_1 > \alpha_2 > \beta > \gamma > \delta$. The *PR* illustrated in Figure 20-B is extended as shown in Figure 24-I. One gets a vertex v surrounded by α_2 and γ in adjacent positions. By the relation between angles the valency of the vertex v is bigger than four. And in order to fulfill the angle-folding relation we must have $\alpha_2 + k\delta = \pi$ for some $k \geq 2$ (Figure 24-II). Now, regarding to the length sides, the alternated angle sum at the vertex v containing γ must be $\gamma + k\delta = \pi$ ($k \geq 2$). Consequently $\alpha_2 = \gamma$, which is a contradiction.
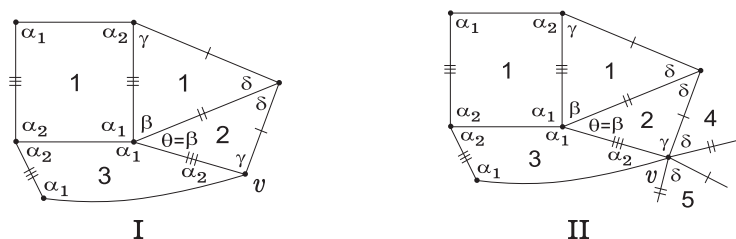
Fig. 24. Planar representations.

ii) Suppose that $\theta = \delta$ and consider firstly that $\alpha_1 + \delta = \pi$ (Figure 25). One gets $\alpha_1 + \delta = \pi = \beta + \delta$, in order to obey the angle-folding relation. With

Fig. 25. Planar representation.

the labelling indicated in this figure, we have $\phi \neq \delta$. And so $\beta + \phi > \pi$, which is an absurd.

Suppose now that $\alpha_1 + \delta < \pi$, as illustrated in Figure 26-I. Using the labelling of this figure, it must be $\theta_1 = \alpha_2$ or $\theta_1 = \delta$. If $\theta_1 = \alpha_2$, then $\gamma > \alpha_2$ (because $\beta + \alpha_2 + \delta \leq \pi < \beta + \gamma + \delta$), and so $\alpha_1 + k\delta = \pi$ for some $k \geq 2$. By considering the length sides of T and Q, we can easily arrive at a contradiction. And so $\theta_1 = \delta$. On the other hand, θ_2 is also δ because the alternated angle sum containing α_1 contains θ_2. Now, using similar argumentation, we conclude that $\theta_3 = \delta$ and so on. Finally, we obtain $\alpha_1 + t\delta = \pi$ and $\beta + t\delta = \pi$ ($t \geq 2$) as the alternated angle sums around this vertex (Figure 26-II). One gets a vertex surrounded by angles β and α_2 in adjacent positions. Regarding to the length sides, in order to obey the angle-folding relation, this vertex must be surrounded by $(\beta, \alpha_2, \gamma, \gamma)$ in cyclic order with $\beta + \gamma = \pi = \alpha_2 + \gamma = \pi$. And so $\alpha_1 = \beta = \alpha_2$, which is an absurd.   □

Fig. 26. Planar representations.

PROPOSITION 3.2. *Let $\tau \in \Omega(Q, T)$ such that τ has two cells in adjacent positions as illustrated in Figure 20-C. Then τ has six cells in adjacent positions as illustrated in Figure 27.*

Fig. 27. Planar representation.

PROOF. Suppose that there are two cells in adjacent positions as illustrated in Figure 20-C. With the labelling of Figure 28-I, let θ_1 and θ_2 be the angles of the tiles adjacent to the triangle 1, such that γ and θ_1 are adjacent angles as well as δ and θ_2.

Fig. 28. Planar representations.

Taking in account the length sides of T, we may conclude that $\theta_1 = \beta$ or $\theta_1 = \gamma$.

If $\theta_1 = \beta$, then $\alpha_1 + \beta = \pi$ (otherwise $\alpha_1 + \beta < \pi < \alpha_1 + \beta + \rho$ for any $\rho \in \{\alpha_1, \alpha_2, \beta, \gamma, \delta\}$). Now the alternated angle sum containing γ cannot be defined, since $\gamma + \rho < \pi$ for any $\rho \in \{\alpha_1, \alpha_2, \beta, \gamma, \delta\}$. Consequently $\theta_1 = \gamma$ and the *PR* illustrated in Figure 28-I is extended as shown in Figure 28-II.

If $\alpha_1 + \theta_1 = \alpha_1 + \gamma < \pi$, then $\beta > \alpha_1$ (because δ is the least angle, and then $\alpha_1 + \gamma + \delta \leq \pi < \beta + \gamma + \delta$). Hence we have no way to set up the tile 3, which is an absurd. Consequently $\alpha_1 + \gamma = \pi$. And so $\theta_2 \in \{\beta, \delta\}$.
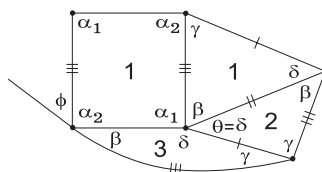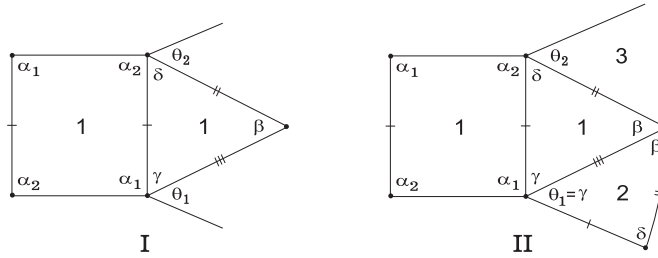
Suppose now, that $\theta_2 = \beta$ and $\alpha_2 + \beta = \pi$. Taking in account the length sides of Q and T, we must have $\alpha_2 + \beta = \pi = \delta + \beta$, which is impossible, since $\alpha_2 > \delta$. The case $\alpha_2 + \beta < \pi$ also leads to a contradiction (note that $\alpha_2 + \beta + \rho \geq \alpha_2 + \beta + \delta > \gamma + \beta + \delta > \pi$ for any $\rho \in \{\alpha_1, \alpha_2, \beta, \gamma, \delta\}$). And so $\theta_2 = \delta$.

The *PR* illustrated in Figure 28-II is now extended to the one represented before (Figure 27). It follows immediately that $\beta = \frac{\pi}{2}$. ☐

PROPOSITION 3.3. *If the PR illustrated in Figure 27 is "contained" in a complete PR of any element $\tau \in \Omega(Q, T)$, then*

$$\tau = \mathscr{M}_{\alpha_2}^3, \qquad \alpha_2 \in \left]\frac{\pi}{3}, \frac{2\pi}{3}\right[, \qquad \alpha_2 \neq \frac{\pi}{2},$$

where $\alpha_1 = \frac{2\pi}{3}$, $\beta = \frac{\pi}{2}$, $\gamma = \frac{\pi}{3}$, $\alpha_2 + 2\delta = \pi$ and the angles around vertices are of the form (with 24 triangles and 6 quadrangles).

Fig. 29. Distinct classes of congruent vertices.

A planar representation of $\mathcal{M}_{\alpha_2}^3$ is given in Figure 32. *Also* 3D *representations are given in Figure* 36.

PROOF.   We shall consider the cases $\alpha_2 \geq \frac{\pi}{2}$ and $\alpha_2 < \frac{\pi}{2}$ separately.
A)   Assume firstly that $\alpha_2 \geq \frac{\pi}{2}$, then

$$\delta < \gamma < \beta = \frac{\pi}{2} \leq \alpha_2 < \alpha_1. \tag{3.1}$$

Let θ be the angle of the tile 6, indicated in Figure 30.
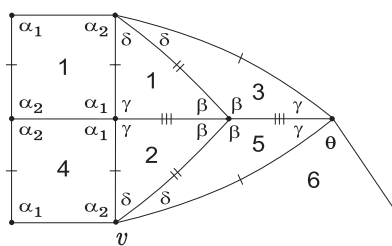
Fig. 30. Planar representation.

One has $\alpha_2 + \gamma + \delta \geq \beta + \gamma + \delta > \pi = \alpha_1 + \gamma > \alpha_2 + \gamma \geq \beta + \gamma$. Thus by (3.1) we conclude that $\theta \in \{\delta, \alpha_1, \gamma\}$.

i)   If $\theta = \delta$, then with the labelling of the refereed Figure, the cyclic sequence of angles around v is of the form $(\alpha_2, \delta, \delta, \gamma, \varepsilon, \ldots)$, where $\varepsilon \geq \gamma$. Consequently the alternated angle sum containing α_2 at the vertex v must be $\alpha_2 + \delta + \varepsilon + \cdots \geq \beta + \delta + \gamma > \pi$, which is a contradiction.

ii)   If $\theta = \alpha_1$, then vertex v is surrounded by $(\alpha_2, \delta, \delta, \alpha_2, \delta, \ldots)$ in cyclic order such that $\alpha_2 + k\delta = \pi$ for some $k \geq 2$ (Figure 31-I). A vertex sur-
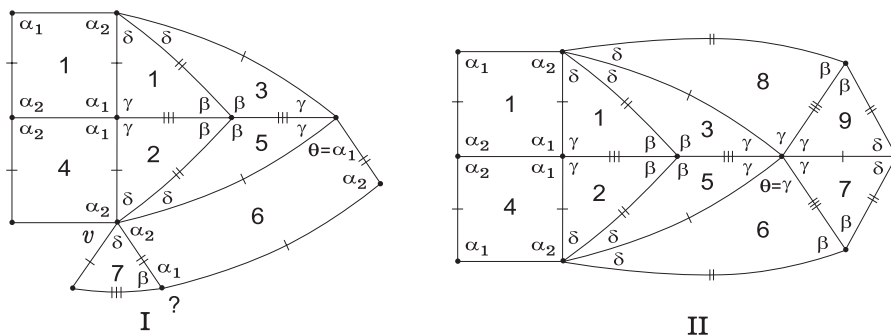
Fig. 31. Planar representations.

rounded by adjacent angles α_1 and β, where the angle-folding relation cannot be fulfilled, takes place.

iii)   Finally we shall suppose that $\theta = \gamma$. With similar argumentation to the one given before, we conclude that the tile 8 (Figure 31-II) is completely determined, and so $\gamma + \gamma + \gamma \leq \pi$. As $\beta = \frac{\pi}{2}$, we have $\gamma + \delta > \frac{\pi}{2}$. Therefore $\gamma = \frac{\pi}{3}$, leading us to the construction represented in Figure 31-II.

Having in consideration (3.1), we must have $\alpha_2 + t\delta = \pi$ for some $t \geq 2$. Since $\alpha_2 \geq \frac{\pi}{2}$, we have $\delta \leq \frac{\pi}{2t}$. Now, $\frac{\pi}{2} < \gamma + \delta \leq \frac{\pi}{3} + \frac{\pi}{2t}$ and so $t = 2$, allowing the extension of the above PR and we obtain the one illustrated in Figure 32. The alternated angle sum around vertices are of the form

$$\alpha_1 + \gamma = \pi, \qquad 2\beta = \pi, \qquad 3\gamma = \pi \qquad \text{and} \qquad \alpha_2 + 2\delta = \pi.$$
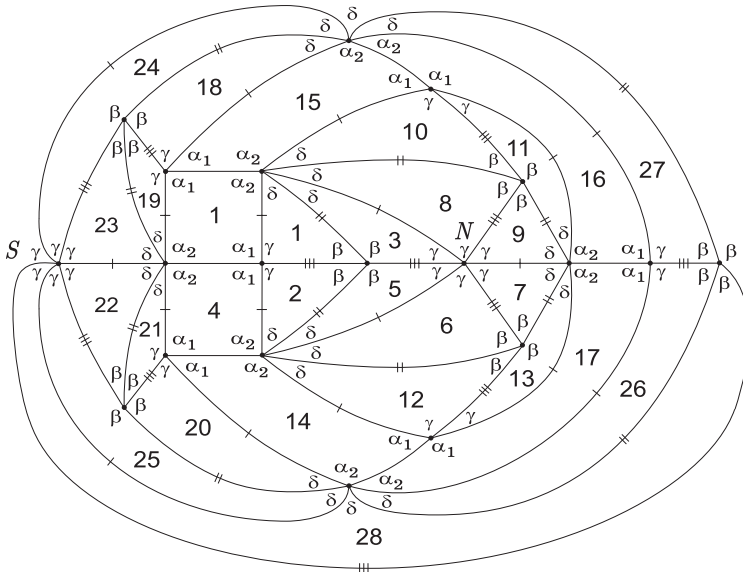
Fig. 32.   Extended planar representation.

The vertices N and S (Figure 32) of valency six and surrounded by angles γ exclusively are in antipodal positions. The extended PR is composed of 6 spherical moons with vertices N and S. Each spherical moon has 4 triangles and 1 quadrangle at its center.

Let $A(Q)$ denote the area of Q. Then

$$0 < A(Q) < \frac{2\pi}{3} \qquad \text{i.e.} \qquad \frac{\pi}{3} < \alpha_2 < \frac{2\pi}{3} \qquad \left(\text{or } \frac{\pi}{6} < \delta < \frac{\pi}{3} \right).$$

It was established in [3] that Q has all congruent sides iff $\alpha_2 = \frac{\pi}{2}$. On the other hand we are considering $\alpha_2 \geq \frac{\pi}{2}$. Therefore $\frac{\pi}{2} < \alpha_2 < \frac{2\pi}{3}$.

    B) Suppose now that $\alpha_2 < \frac{\pi}{2}$. One has $\alpha_1 + \alpha_2 > \pi$, $\beta = \frac{\pi}{2}$ and $\alpha_1 + \gamma = \pi$. Therefore

$$\alpha_1 > \beta > \alpha_2 > \gamma > \delta \tag{3.2}$$

and also $\gamma + \delta > \frac{\pi}{2}$. The alternated angle sum containing α_2 at the vertex v (or v') (Figure 27, Page 17) must satisfy one of the following conditions:

  i) $\alpha_2 + \delta + \alpha_2 = \pi$;   ii) $\alpha_2 + \delta + \gamma = \pi$;   iii) $\alpha_2 + k\delta = \pi$, $k \geq 2$.

    i) Suppose firstly that the alternated angle sum containing α_2 at the vertex v is $\alpha_2 + \delta + \alpha_2 = \pi$. Therefore the cyclic sequence of angles around v is of the form

$$(\alpha_2, \delta, \delta, \theta_1, \alpha_2, \theta_2), \qquad \text{where } \alpha_2 + \delta + \alpha_2 = \pi = \delta + \theta_1 + \theta_2.$$

Taking in account the length sides of Q and T, we may conclude that

$$(\theta_1, \theta_2) = (\alpha_1, \delta) \qquad \text{or} \qquad (\theta_1, \theta_2) = (\alpha_2, \alpha_2).$$

    The first case is illustrated in Figure 33-I. With this choice of angles one gets a vertex surrounded by α_1, β and γ in adjacent positions, where we have no way to fulfill the angle-folding relation.

    The second case is presented in Figure 33-II. With the labelling of this Figure, we have $\tilde{\theta}_1 \neq \delta$. In fact, if $\tilde{\theta}_1 = \delta$, then v_1 is surrounded by the cyclic

Fig. 33. Planar representations.

sequence $(\alpha_1, \alpha_1, \delta, \delta, \delta, \delta, \ldots)$, $\alpha_1 + k\delta = \pi$ for some $k \geq 2$. Hence $\gamma = k\delta$. On the other hand the alternated angle sum at the vertex w_1 must obey $\alpha_2 + \gamma + \gamma = \pi$ (because it contains the angles α_2 and γ, $\alpha_2 + \gamma + \delta < \pi = 2\alpha_2 + \delta$ and w_1 has valency six). Therefore $\gamma < \frac{\pi}{3}$, since $\alpha_2 > \gamma$. Now $\gamma + \delta = \gamma + \frac{\gamma}{k} < \frac{\pi}{3} + \frac{\pi}{6} = \frac{\pi}{2}$ that is an absurd. Consequently $\tilde{\theta}_1 = \gamma$, as illustrated in refereed Figure. This information leads us to obtain a vertex surrounded by the cyclic sequence of angles $(\beta, \alpha_2, \delta, \delta, ?)$. Taking in account that Q has distinct pairs of opposite sides, the angle-folding relation fails at this vertex.

ii) Suppose now that the alternated angle sum containing α_2 at the vertex v is $\alpha_2 + \delta + \gamma = \pi$. It is a straightforward exercise to show that the cyclic sequence of angles around v must be the one illustrated below—Figure 34-I (it is enough to use (3.2) and the length sides of the prototiles).

This extension leads to a vertex v_2 surrounded by the cyclic sequence of angles $(\alpha_1, \delta, \delta, \tilde{\theta}_2, \delta, \ldots)$ such that $\alpha_1 + t\delta = \pi$ for some $t \geq 2$ and $\tilde{\theta}_2 \in \{\alpha_1, \alpha_2, \delta\}$. Considering firstly that $\tilde{\theta}_2 = \alpha_1$, then we get a vertex w_2 such that β and α_2 are in adjacent positions and similar to the previous case we have no way to fulfill the angle-folding relation around w_2. The case $\tilde{\theta}_2 = \alpha_2$ leads also to an absurd (Proposition 3.1). In Figure 34-II we illustrate the case $\tilde{\theta}_2 = \delta$.
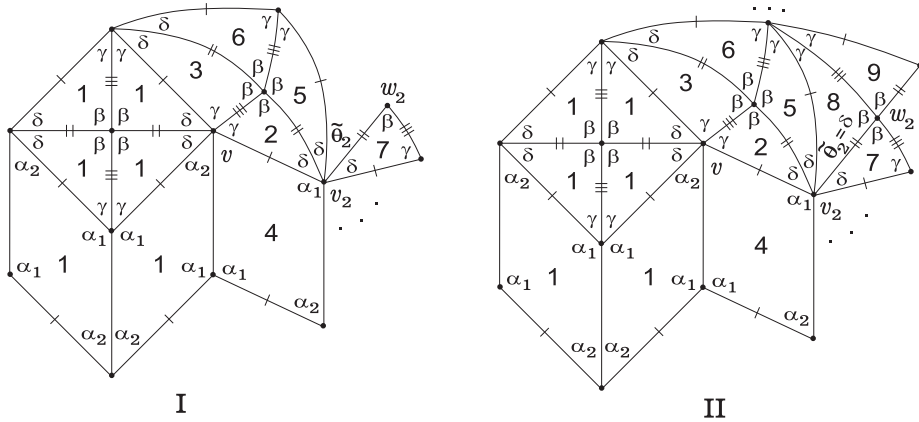

Fig. 34. Planar representations.

This procedure gives rise to a vertex surrounded by the sequence of angles $(\gamma, \gamma, \gamma, \gamma, \ldots)$ as illustrated in refereed Figure. As $2\gamma + \alpha_2 > \alpha_2 + \delta + \gamma = \pi$ and $\gamma + \delta > \frac{\pi}{2}$, we must have $\gamma = \frac{\pi}{3}$. On the other hand $\alpha_1 + \gamma = \pi$ and so $\alpha_1 = \frac{2\pi}{3}$. Therefore $\delta \leq \frac{\pi}{6}$, since $\alpha_1 + t\delta = \pi$ for some $t \geq 2$ (vertex v_2). Now, $\beta + \gamma + \delta \leq \frac{\pi}{2} + \frac{\pi}{3} + \frac{\pi}{6} = \pi$, which is an absurd.

iii) Finally we shall suppose that the alternated angle sum containing α_2 at the vertex v (Figure 27, Page 17) is $\alpha_2 + k\delta = \pi$ for some $k \geq 2$.

Using the labelling of Figure 35-I, one has $\theta \neq \alpha_2$ (as seen in Proposition 3.1) and obviously $\theta \neq \alpha_1$. And so $\theta = \delta$ (see length sides). Applying the same kind of reasoning around the vertex v, we may conclude that v is surrounded by the cyclic sequence of angles $(\alpha_2, \delta, \delta, \delta, \delta, \ldots, \alpha_2)$, $\alpha_2 + k\delta = \pi$ for some $k \geq 2$. The same occurs around vertex v', leading us to extend this PR to the one as illustrated in Figure 35-II. We may also conclude that $\gamma = \frac{\pi}{3}$ and consequently $\alpha_1 = \frac{2\pi}{3}$, since $\alpha_1 + \gamma = \pi$.
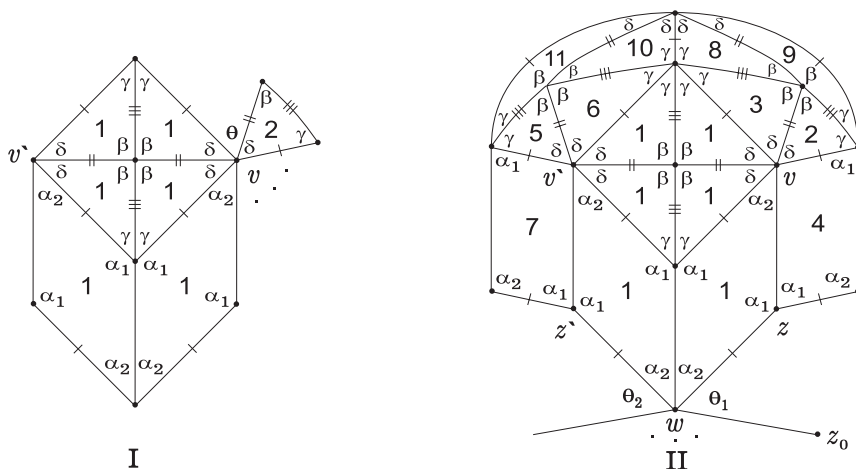

Fig. 35. Planar representations.

Now using the labelling of Figure 35-II, the valency of w is bigger than four. Let us verify that the vertex w can not contain the angle γ. In fact if w contains the angle γ, then $\alpha_2 + \gamma + \delta = \pi$, and necessarily $\theta_1 = \gamma$ or $\theta_2 = \gamma$ (see length sides). Considering for instance $\theta_1 = \gamma$, one gets a vertex with angles α_1 and δ in adjacent positions. Hence we must have $\alpha_1 + n\delta = \pi$ for some $n \geq 2$. As $\alpha_1 = \frac{2\pi}{3}$, we have $\delta = \frac{\pi}{3n} \leq \frac{\pi}{6}$. Consequently $\beta + \gamma + \delta \leq \frac{\pi}{2} + \frac{\pi}{3} + \frac{\pi}{6} = \pi$, which is a contradiction. It follows that the alternated angle sum at the vertex w must be of the form $2\alpha_2 + \delta = \pi$ or $\alpha_2 + k\delta = \pi$ $(k \geq 2)$, by using the condition (3.2). On the other hand w cannot be surrounded by the cyclic sequence of angles $(\alpha_2, \alpha_2, \delta, \alpha_2, \alpha_2, \delta)$ (otherwise, the vertex z_0 must be surrounded by α_1 and β in adjacent positions, leading us to an absurd (by Proposition 3.1 (Page 14) or, by using the length sides around z_0)). The possibilities $(\alpha_2, \alpha_2, \delta, \delta, \alpha_2, \alpha_2)$, $(\alpha_2, \alpha_2, \alpha_2, \delta, \delta, \alpha_2)$ and $(\alpha_2, \alpha_2, \alpha_2, \alpha_2, \delta, \delta)$ lead to one of the vertices z or z' to be surrounded by three angles α_1, which is not possible. Thus, we conclude that the cyclic sequence of angles around w must be $(\alpha_2, \alpha_2, \delta, \delta, \delta, \delta, \ldots)$ $(k \geq 2)$.

In order to determine k we proceed as follows: One has $\alpha_1 = \frac{2\pi}{3}$, $\gamma = \frac{\pi}{3}$, $\beta = \frac{\pi}{2}$ and $\alpha_2 + k\delta = \pi$, $\gamma < \alpha_2 < \beta$ for some $k \geq 2$. On the other hand $\gamma + \delta > \frac{\pi}{2}$. Therefore $\frac{\pi}{6} < \delta < \frac{2\pi}{3k}$. And so $k = 2$ or $k = 3$.

Consider firstly that $k = 3$. Under these conditions the PR illustrated in Figure 35-II is extended in a unique way to a complete PR of a dihedral f-tiling, in which all the angles are completely determined. In fact one gets $\alpha_1 = \frac{2\pi}{3}$, $\alpha_2 = \frac{2\pi}{5}$, $\beta = \frac{\pi}{2}$, $\gamma = \frac{\pi}{3}$ and $\delta = \frac{\pi}{5}$, which implies that Q has all congruent sides. This f-tiling was denoted by $\mathscr{G}_3$ (see [3] for a detailed study).

Suppose then that $k = 2$. In this case the previous PR (Figure 35-II) is uniquely extended to a PR with the same configuration as the one illustrated in Figure 32 (Page 20), where $\frac{\pi}{3} < \alpha_2 < \frac{\pi}{2}$ (or $\frac{\pi}{4} < \delta < \frac{\pi}{3}$). $\qquad\square$

REMARK. In Figure 36 3D representations of $\mathscr{M}^3_{\alpha_2}$ $\left(\frac{\pi}{3} < \alpha_2 < \frac{2\pi}{3}\right)$ are illustrated. It is composed of 24 triangles and 6 quadrangles. The limit case $\alpha_2 = \frac{\pi}{3}$ leads to a monohedral f-tiling ([4], [11]), where the prototile is an isosceles triangle of angles $\frac{\pi}{2}$, $\frac{\pi}{3}$ and $\frac{\pi}{3}$. Observe that $\mathscr{M}^3_{\alpha_2}$ is obtained from $\mathscr{R}^3_{\alpha_2}$ (Page 8), by adding some edges, bisecting any triangle of $\mathscr{R}^3_{\alpha_2}$ and preserving the angle-folding relation.

$$\frac{\pi}{3} < \alpha_2 < \frac{\pi}{2} \qquad\qquad\qquad\qquad \frac{\pi}{2} < \alpha_2 < \frac{2\pi}{3}$$
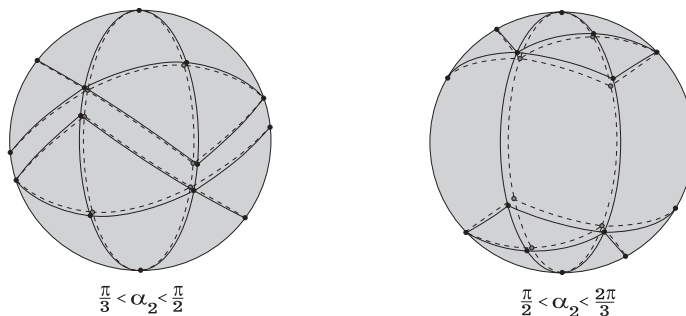
Fig. 36. 3D representations.

PROPOSITION 3.4. *Let $\tau \in \Omega(Q, T)$ such that τ has two cells in adjacent positions as illustrated in Figure 20-D. Then τ has six cells in adjacent positions as illustrated in Figure 37.*

PROOF. Suppose that there are two cells in adjacent positions as illustrated in Figure 20-D. With the labelling of Figure 38-I, it follows immediately that $\theta_1 \in \{\beta, \delta\}$ and $\theta_2 \in \{\beta, \alpha_2, \gamma\}$.

If $\theta_1 = \beta$, then we have necessarily $\alpha_1 + \beta = \pi$. The case $\alpha_1 + \beta < \pi$ leads to a contradiction as seen in the proof of Proposition 3.1—Case A) i). The alternated angle sum containing δ is of the form $\delta + \rho < \pi$, for all $\rho \in \{\alpha_1, \alpha_2, \beta, \gamma, \delta\}$, leading us to a contradiction. And so $\theta_1 = \delta$.
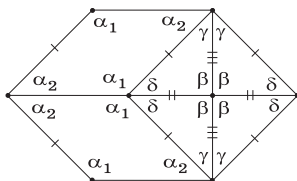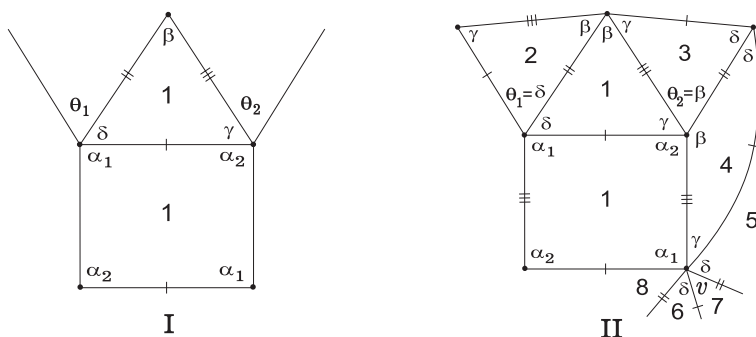
Fig. 37. Planar representation.

Fig. 38. Planar representations.

i) Let us suppose now that $\theta_2 = \beta$. Analyzing the length sides of Q and T, we conclude that, if $\alpha_2 + \beta = \pi$, then $\alpha_2 + \beta = \pi = \gamma + \beta$ as illustrated in Figure 38-II. It follows that $\alpha_1 > \beta > \frac{\pi}{2} > \gamma = \alpha_2 > \delta$. Now, considering a vertex v in which α_1 and γ are in adjacent positions, we must have $\alpha_1 + k\delta = \gamma + k\delta$ $(k \geq 1)$ in order to fulfill the angle-folding relation around v. Thus $\alpha_1 = \gamma$, which is an absurd.

Suppose now that $\alpha_2 + \theta_2 = \alpha_2 + \beta < \pi$ (Figure 39). Then $\alpha_1 > \beta > \gamma > \alpha_2 > \delta$. (In fact, the relation $\alpha_1 + \delta \leq \pi < \alpha_1 + \alpha_2$ implies $\alpha_2 > \delta$. On the other hand since δ is the least angle, we must have $\alpha_2 + \beta + \delta \leq \pi < \beta + \gamma + \delta$ and so $\gamma > \alpha_2$. $\alpha_1 > \beta$ holds from the fact $\alpha_2 + \beta < \pi < \alpha_1 + \alpha_2$.) Now, from the PR it follows that $\beta + \gamma = \pi$. First consider the alternated angle sum containing $\alpha_2 + \beta$. Since $\alpha_2 + \beta + \gamma > \beta + \gamma + \delta > \pi$, the remaining angles must be α_2 or δ. Similarly, the alternated angle sum containing γ must be of the form $p\gamma + q\alpha_2 + r\delta$. In any case, this vertex does not contain more angles β. Hence the adjacent edges around this vertex cannot be those of the angle β, including the case of quadrangles. Then the edges between two angles γ and δ appear alternately around this vertex, because the adjacent edges must have different lengths, and also it cannot be those of the angle β, as stated above. Then by an elementary combinatorial argument, we can easily arrive at a contradiction since the valency of this vertex is even.
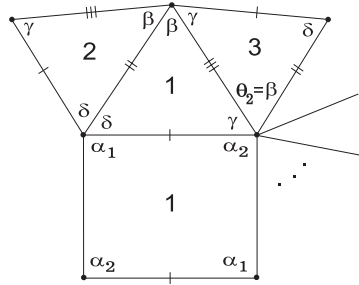
Fig. 39. Planar representation.

ii) Consider now that $\theta_2 = \alpha_2$. In this case the *PR* illustrated in Figure 38-I is extended as follows (Figure 40-I). One has α_1 and β in adjacent positions. By Proposition 3.1 we get an absurd.
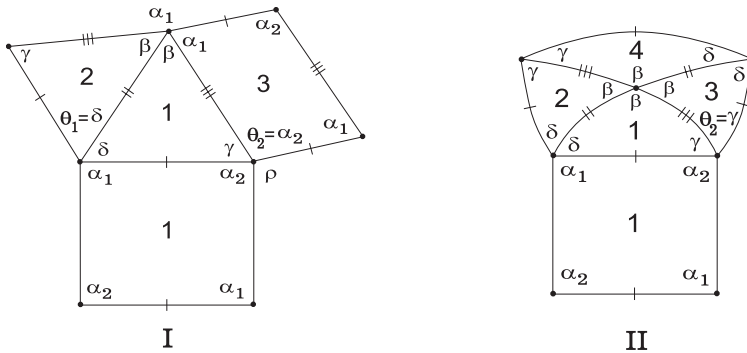

Fig. 40. Planar representations.

iii) Finally we shall suppose that $\theta_2 = \gamma$ (Figure 40-II). It follows straightway that $\beta = \frac{\pi}{2}$.

In order to prove $\alpha_1 + \delta = \pi$, we shall consider two cases separately:

    (1) $\alpha_1 + \delta < \pi$ and $\alpha_2 + \gamma = \pi$ (2) $\alpha_1 + \delta < \pi$ and $\alpha_2 + \gamma < \pi$

and we will show that both cases lead us to a contradiction.

(1) Assume that $\alpha_1 + \delta < \pi$ and $\alpha_2 + \gamma = \pi$. As $\beta = \frac{\pi}{2}$, we have $\alpha_1 > \alpha_2 > \beta > \gamma > \delta$, and so $\alpha_1 + k\delta = \pi$ for some $k \geq 2$. The previous *PR* (Figure 40-II) is uniquely extended as shown in Figure 41.

One gets a vertex v_1 surrounded by four γ angles. In order to fulfill the angle-folding relation at v_1 we must have $2\gamma + \delta = \pi$ or $3\gamma = \pi$. On the other hand, the vertex v_2 cannot be surrounded by γ, therefore v_1 must be surrounded
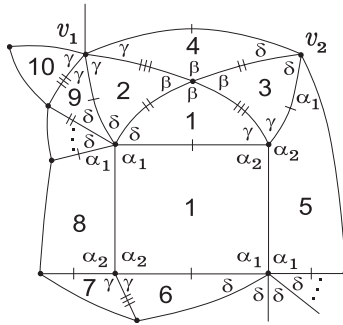
Fig. 41. Planar representation.

by six angles γ and so $\gamma = \frac{\pi}{3}$. Now, one gets $\alpha_1 > \alpha_2 = \frac{2\pi}{3}$, and as $\alpha_1 + k\delta = \pi$ for some $k \geq 2$, then $\delta < \frac{\pi}{6}$. Consequently $\beta + \gamma + \delta < \frac{\pi}{2} + \frac{\pi}{3} + \frac{\pi}{6} = \pi$, which is an absurd.

(2) Assume now that $\alpha_1 + \delta < \pi$ and $\alpha_2 + \gamma < \pi$. Since δ is the least angle, we have $\alpha_2 + \gamma + \delta \leq \pi$. But, $\beta + \gamma + \delta > \pi$, and so $\beta > \alpha_2$. We shall discern the cases $\alpha_2 \geq \gamma$ and $\alpha_2 < \gamma$.

If $\alpha_2 \geq \gamma$, then $\alpha_1 > \beta = \frac{\pi}{2} > \alpha_2 \geq \gamma > \delta$ and so $\alpha_1 + t\delta = \pi$ for some $t \geq 2$. One has $(\alpha_2 + 2\gamma) + (\alpha_1 + t\delta) = (\alpha_2 + \alpha_1) + (2\gamma + t\delta) > 2\pi$, for some $t \geq 2$. Therefore $\alpha_2 + 2\gamma > \pi$, and so $\alpha_2 + \gamma + \delta = \pi$. Taking in account the length sides of the prototiles and by using Proposition 3.1 (Page 14), the *PR* illustrated in Figure 40-II is uniquely extended as illustrated below (see Figure 42).
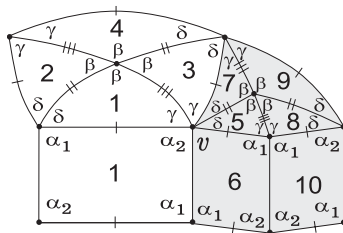

Fig. 42. Planar representation.

Now, as seen in the proof of Proposition 3.3 (Figure 32), the vertex v (as vertex of the dark portion) cannot be surrounded by γ, leading us in this way to a contradiction.

If $\alpha_2 < \gamma$, then

$$\alpha_1 > \beta = \frac{\pi}{2} > \gamma > \alpha_2 > \delta. \tag{3.3}$$

And, hence $\alpha_1 + t\delta = \pi$ for some $t \geq 2$. Now, one has:

(a) Since Q has distinct pairs of opposite sides, and since α_1 and β cannot be in adjacent positions (Proposition 3.1), we have $\theta \neq \gamma$ and $\theta \neq \delta$ (Figure 43-I). We immediately conclude that $\theta = \alpha_2$, leading to the extension illustrated in Figure 43-II.

(b) As before, we have $\alpha_2 + 2\gamma > \pi$, and so $\theta' \neq \gamma$. On the other hand, we have $\theta' \neq \delta$ (otherwise, the alternated angle sum containing α_1 at the vertex z (Figure 43-II) cannot be defined, by using the length sides and (3.3)). And so $\theta' = \alpha_2$.
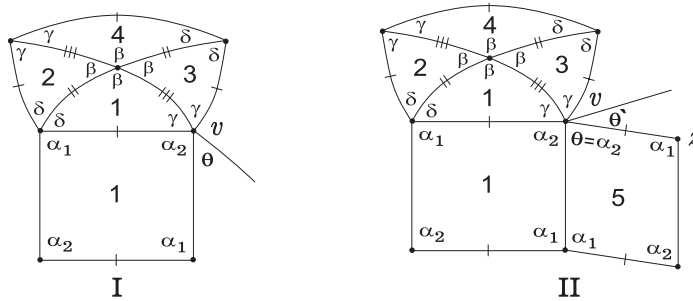

Fig. 43. Planar representations.

Using alternately (a) and (b) around the vertex v, we conclude that v has to be surrounded by the cyclic sequence $(\gamma, \gamma, \alpha_2, \alpha_2, \alpha_2, \alpha_2, \ldots)$ with $\gamma + k\alpha_2 = \pi$ ($k \geq 2$), allowing us to extend the last PR as shown in Figure 44. In fact, by (3.3) tiles labelled 8 are uniquely determined. On the other hand, the angle ε (tile 9) adjacent to α_2 is also α_2. Clearly it is not α_1, by using (3.3). If it is β, then $\beta + \gamma < \pi$ and by adding the least angle, it exceeds π. An argumentation as the one used in (a) shows that $\varepsilon \neq \gamma$ and $\varepsilon \neq \delta$. And so $\varepsilon = \alpha_2$, as indicated in Figure 44. With similar argumentation one gets a vertex w_1 surrounded by four angles γ. As $\gamma + \delta > \frac{\pi}{2}$ and $3\gamma > 2\gamma + \alpha_2 > \pi$, we have $2\gamma + \delta = \pi$ as illustrated in refereed Figure. A vertex w_2 surrounded by the cyclic sequence of angles $(\alpha_1, \delta, \delta, \gamma, \ldots)$ must take place, leading us to a contradiction, since there is no way to position other cells around w_2 in order to fulfill the angle-folding relation.

The PR illustrated in Figure 38-I (or Figure 20-D) is now extended to get the one represented in Figure 37, where $\alpha_1 + \delta = \pi$, $\beta = \frac{\pi}{2}$ and $\alpha_2 + \gamma \leq \pi$. $\qquad\square$

PROPOSITION 3.5. *Suppose that the PR illustrated in Figure 37 is contained in a complete PR of any element $\tau \in \Omega(Q, T)$.*
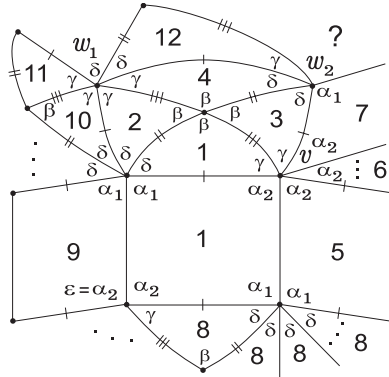
Fig. 44. Planar representation.

i)   If $\alpha_2 + \gamma < \pi$, then $\tau = \mathcal{M}_{\alpha_2}^k$, $\frac{\pi}{k} < \alpha_2 < \frac{2\pi}{k}$ ($\alpha_2 \neq \arccos(2\cos(\pi/k) - 1) = \alpha_2^k$), $k \geq 4$, where $\alpha_1 = \pi - \frac{\pi}{k}$, $\beta = \frac{\pi}{2}$, $\gamma = \frac{\pi - \alpha_2}{2}$ and $\delta = \frac{\pi}{k}$;

ii) If $\alpha_2 + \gamma = \pi$, then $\tau = \mathcal{R}_{\gamma\delta}^2$, where $\alpha_1 + \delta = \pi$ and $\beta = \frac{\pi}{2}$. The angles γ and δ obey, $\cos\gamma = \frac{\sqrt{2}}{2}\left(\sin\frac{\theta}{2} - \cos\frac{\theta}{2}\sin x\right)$ and $\cos\delta = \frac{\sqrt{2}}{2}\left(\sin\frac{\theta}{2} + \cos\frac{\theta}{2}\sin x\right)$ for some $x \in\,]0, \frac{\pi}{2}[$ and $\theta \in\,]2\arctan(\sin x), \pi[\setminus\{\frac{\pi}{2}\}$. (In particular $\frac{\pi}{4} < \gamma < \frac{\pi}{2}$, $0 < \delta \leq \frac{\pi}{2}$ ($\delta < \gamma$) and $\cos\gamma + \cos\delta < \sqrt{2}$ ($\neq 1$).)

The angles around vertices are positioned as illustrated in Figure 45.
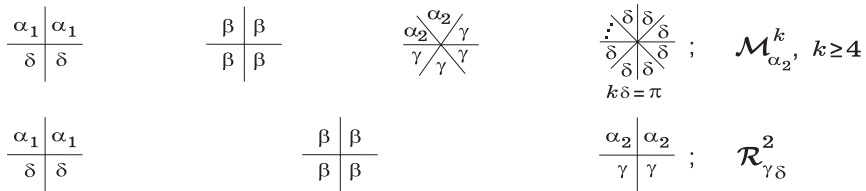
Fig. 45. Distinct classes of congruent vertices.

3D representations of $\mathcal{M}_{\alpha_2}^k$ and $\mathcal{R}_{\gamma\delta}^2$ are given in Figure 47, and Figure 49-II, respectively.

PROOF.   i) Suppose that $\alpha_2 + \gamma < \pi$.   As $\alpha_1 + \delta = \pi$ and $\beta = \frac{\pi}{2}$, we have $\alpha_1 > \beta > \alpha_2 > \delta$ and $\beta > \gamma > \delta$.   Starting from the *PR* illustrated in Figure 37 (labelled 1), we extend in a unique way such *PR* to the one illustrated in Figure 46. Vertices surrounded by $(\alpha_2, \alpha_2, \gamma, \gamma, \gamma, \gamma)$, $\alpha_2 + 2\gamma = \pi$ are forced to take place.   Besides, there are two vertices surrounded by angles δ exclusively. Hence, there exists k such that $k\delta = \pi$.
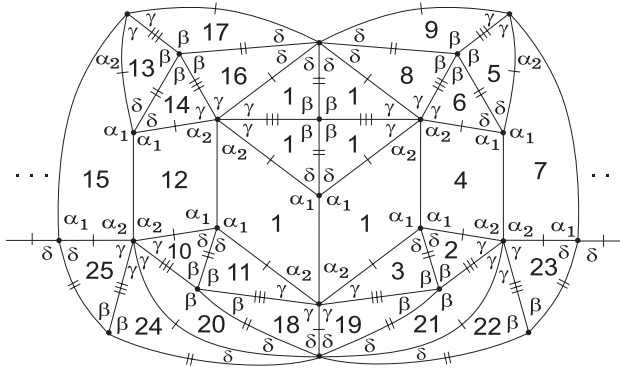
Fig. 46. Planar representation.

For any $k \geq 4$ we may "close" this PR, obeying the angle-folding relation (if $k = 3$, then $\delta = \frac{\pi}{3}$ and so $\alpha_2 + 2\gamma > \pi$ because $\alpha_2, \gamma > \delta$), where the alternated angle sum at vertices are

$$\alpha_1 + \delta = \pi, \qquad 2\beta = \pi, \qquad \alpha_2 + 2\gamma = \pi \qquad \text{and} \qquad k\delta = \pi.$$

An extended PR can be also obtained from the PR illustrated in Figure 9 (Page 8, Proposition 2.2), bisecting through β any isosceles triangle of $\mathscr{R}_{\alpha_2}^k$ $\left(\frac{\pi}{k} < \alpha_2 < \frac{2\pi}{k}\right)$. Such f-tilings are denoted by $\mathscr{M}_{\alpha_2}^k$, $\frac{\pi}{k} < \alpha_2 < \frac{2\pi}{k}$ and are composed of $8k$ triangles and $2k$ quadrangles.

For any $k \geq 3$ a 3D representation of $\mathscr{M}_{\alpha_2}^k$ is then obtained from a 3D representation of $\mathscr{R}_{\alpha_2}^k$ (Figure 10), by adding some edges splitting asunder any triangle of $\mathscr{R}_{\alpha_2}^k$ and preserving the angle-folding relation (the case $k = 3$ is in Proposition 3.3). 3D representations of $\mathscr{M}_{\alpha_2}^k$ ($k = 4$ and $k = 5$) are illustrated in Figure 47.
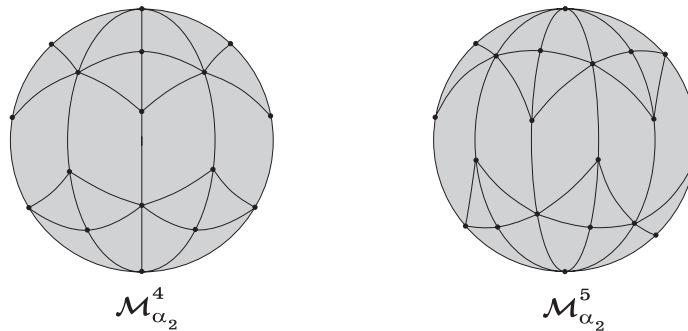
Fig. 47. 3D representations.

As Q has distinct pairs of opposite sides, we have $\alpha_2 \neq \arccos(2\cos(\pi/k) - 1)$ [3]. Note also that if $\alpha_2 = \frac{\pi}{k}$, then one gets a monohedral f-tiling in which the prototile has angles $\frac{\pi}{2} - \frac{\pi}{2k}$, $\frac{\pi}{2}$ and $\frac{\pi}{k}$, established in [4] and [11].

ii) Suppose now that $\alpha_2 + \gamma = \pi$. Then the PR illustrated in Figure 37 (Page 23) is extended in a unique way as shown in Figure 48, where $\alpha_1 + \delta = \pi$, $\beta = \frac{\pi}{2}$ and $\alpha_1 > \alpha_2 > \beta > \gamma > \delta$. Such an f-tiling is denoted by $\mathscr{R}^2_{\gamma\delta}$.

In order to determine γ and δ we proceed as follows: As Q is a spherical quadrangle with distinct pairs of congruent opposite angles and distinct pairs of congruent opposite sides, Q is congruent to a WCSQ* $L_1 \cap L_2$, where L_1 and L_2 are well centered non-orthogonal spherical moons with distinct angle measure θ and θ_1 ($\theta \neq \theta_1$), respectively [1]. The PR illustrated in Figure 48 is composed of four spherical moons with vertices surrounded by β; Each spherical moon has two congruent triangles and one quadrangle at its center. Hence we may suppose that $\theta_1 = \beta = \frac{\pi}{2}$ and $0 < \theta < \pi$, $\theta \neq \frac{\pi}{2}$ (Figure 49-I).
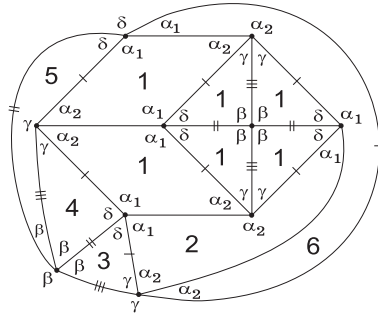
Fig. 48. Planar representation.
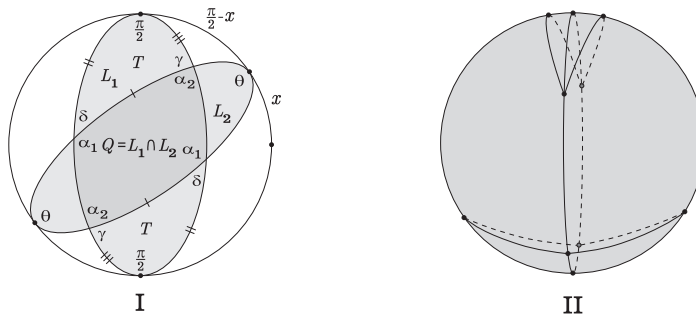
Fig. 49. A WCSQ and a 3D representation of $\mathscr{R}^2_{\gamma\delta}$.

With the labelling of Figure 49-I, one has

$$\cos \gamma = \frac{\sqrt{2}}{2}\left(\sin\frac{\theta}{2} - \cos\frac{\theta}{2}\sin x\right) \qquad \text{and} \qquad \cos \delta = \frac{\sqrt{2}}{2}\left(\sin\frac{\theta}{2} + \cos\frac{\theta}{2}\sin x\right),$$

for some $x \in \left]0,\frac{\pi}{2}\right[$ $\left(x = \frac{\pi}{2} - \angle(L_1, L_2)\right)$ and $\theta \in \left]0,\pi\right[$, $\theta \neq \frac{\pi}{2}$. And so

$$\cos\gamma + \cos\delta = \sqrt{2}\sin\frac{\theta}{2}, \qquad \text{for some } \theta \in \left]0,\pi\right[\backslash\{\pi/2\} \text{ and } \delta < \gamma.$$

Now, for all $x \in \left]0,\frac{\pi}{2}\right[$ we must determine θ such that $\gamma(x,\theta) = \gamma < \frac{\pi}{2} = \beta$. In fact,

$$\gamma < \frac{\pi}{2} \Leftrightarrow \cos\gamma > 0 \Leftrightarrow \sin\frac{\theta}{2} > \cos\frac{\theta}{2}\sin x \Leftrightarrow \theta > 2\arctan(\sin x).$$

It follows that:

- $\forall x \in \left]0,\dfrac{\pi}{2}\right[, \quad \forall \theta \in \left]2\arctan(\sin x),\pi\right[, \qquad \dfrac{\pi}{4} < \gamma < \dfrac{\pi}{2};$

- $\forall x \in \left]0,\dfrac{\pi}{2}\right[, \quad \forall \theta \in \left]2\arctan(\sin x),\pi\right[, \qquad 0 < \delta < \dfrac{\pi}{2}.$

The variation of the functions γ and δ are presented in Figure 50-I and Figure 50-II, respectively. The value of contour level is signalized into a circle. A 3D representation is illustrated in Figure 49-II.

Fig. 50. $\gamma(x,\theta)$ and $\delta(x,\theta)$.

REMARK. Limit cases: Observe that
1. If $x = 0$ and $0 < \theta < \pi$, then $\delta = \gamma$ and so $\alpha_1 = \alpha_2$, which means that Q has all congruent internal angles, giving rise to a family of dihedral f-tilings established in [2]. In addition

(a) if $\theta = \frac{\pi}{2}$, then Q has all congruent sides (and all congruent angles);

(b) if $\theta = 0$, then one gets a monohedral f-tiling ([4], [11]). The prototile is an equilateral spherical triangle with internal angle $\frac{\pi}{2}$.
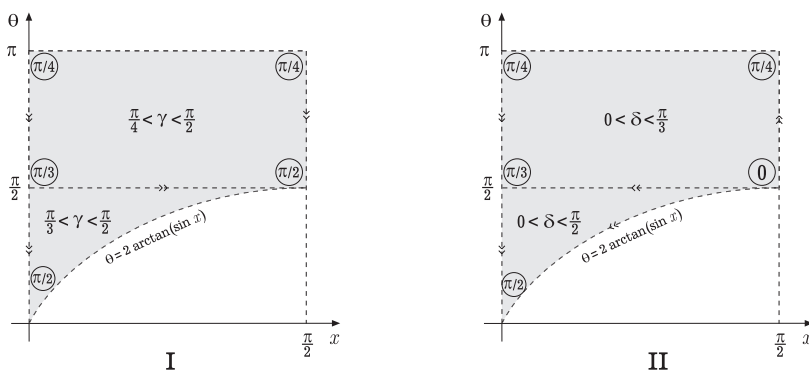
2. If $\theta = \frac{\pi}{2}$ and $0 < x < \frac{\pi}{2}$, then Q has all congruent sides and distinct pairs of opposite angles. Such a family of f-tilings was obtained in [3];

3. If $0 < x < \frac{\pi}{2}$ and $\theta = 2\arctan(\sin x)$, then T is an isosceles triangle with angles $\frac{\pi}{2}$, $\frac{\pi}{2}$, ε, $0 < \varepsilon < \frac{\pi}{2}$. This family of dihedral f-tilings was established in Proposition 2.3 (Page 9) for $k = 1$.

Next we obtain f-tilings $\tau \in \Omega(Q, T)$ coming from the adjacency illustrated in Figure 20-E or Figure 20-F (Page 13). In both cases the angles α_2 and β are in adjacent positions. With the labelling in Figure 51, $(y, z) = (\delta, \gamma)$ or $(y, z) = (\gamma, \delta)$.
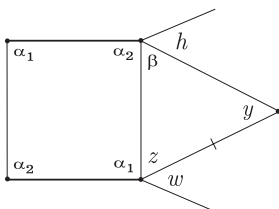
Fig. 51. Planar representation.

PROPOSITION 3.6. *With the above terminology, if $\Omega(Q, T) \neq \varnothing$, then $z = w$, $h \in \{\alpha_2, \beta\}$ and $\alpha_2 + h = \pi$.*

PROOF. We shall distinguish the cases $z = \delta$ and $z = \gamma$.

A) Assume firstly that $z = \delta$ (Figure 52-I). Obviously $w \in \{\gamma, \delta\}$ and $h \in \{\gamma, \beta, \alpha_2\}$.

Consider firstly that $w = \gamma$. Taking in account the length sides of Q, we must have $\alpha_1 + \gamma < \pi$. Hence, it must be $\beta > \alpha_1 > \alpha_2 > \gamma > \delta$. Now, by using the length sides of Q and T, the vertex surrounded by the cyclic sequence of angles $(\alpha_2, \beta, h, \ldots)$ cannot have valency four. Therefore $\beta + k\delta = \pi$ for some $k \geq 2$ (see Figure 52-II). Analyzing the length sides, one gets $h = \beta$. Now, $\alpha_2 + h = \alpha_2 + \beta > \alpha_2 + \alpha_1 > \pi$, which is an absurd. And so $w = \delta = z$.

Consider now that $h = \gamma$. If $\alpha_2 + \gamma = \pi$ (Figure 53-I), then $\alpha_2 + \gamma = \pi = \beta + \gamma$ (according to the length sides). One gets a vertex surrounded by α_1 and β in adjacent positions. By Proposition 3.1 (Page 14) one gets an absurd.

If $\alpha_2 + \gamma < \pi$ (Figure 53-II), then looking at the vertex v_1, we conclude that $\beta + \gamma$ has to be π (note that $\beta + \gamma + \rho > \pi$ for all $\rho \in \{\alpha_1, \alpha_2, \beta, \gamma, \delta\}$). Therefore the alternated angle sum containing β at the vertex v is $\beta + \varepsilon_1 + \varepsilon_2 + \cdots = \pi$,

Fig. 52. Planar representations.

Fig. 53. Planar representations.

where $\varepsilon_i = \alpha_2$ or $\varepsilon_i = \delta$ for all $i \in \{1, 2, \ldots, N\}$, $N \geq 2$. In any case we have no way to avoid an incompatibility between sides as illustrated in refereed Figure. And so $h = \beta$ or $h = \alpha_2$.

 i) Suppose that $h = \beta$. If $\alpha_2 + h = \alpha_2 + \beta < \pi$ (Figure 54-I and 54-II), then

$$\alpha_1 > \beta > \gamma > \alpha_2 > \delta. \tag{3.4}$$

Fig. 54. Planar representations.

Surely the tile 3 is a triangle or a quadrangle. In the first case it must be set up as illustrated in Figure 54-I (observe that the cyclic sequence $(\phi, \alpha_2, \beta, h = \beta, \ldots)$ ($\phi \in \{\gamma, \beta\}$) does not occur, since $\alpha_2 + h < \pi$ and $\phi + \beta + \rho > \pi$ for any $\rho \in \{\alpha_1, \alpha_2, \beta, \gamma, \delta\}$). Thus, one gets a vertex surrounded by α_1 and γ in adjacent positions. By using the relation between angles (3.4) and the length sides of T, the alternated angle sum containing α_1 around this vertex cannot be defined. And hence the tile 3 has to be a quadrangle as illustrated in Figure 54-II. Using similar arguments, the tile labelled by 4 is also a quadrangle. By using the condition (3.4), the tiles 5 and 6 have to be set up as illustrated in refereed Figure. And so a vertex w surrounded by the cyclic sequence $(\beta, \alpha_2, \gamma, \ldots)$ must take place. Analyzing the length sides around w, we conclude that w has valency bigger than four. But, on the other hand $\beta + \gamma + \rho > \pi$ for any $\rho \in \{\alpha_1, \alpha_2, \beta, \gamma, \delta\}$, which is an absurd. And so $\alpha_2 + h = \alpha_2 + \beta = \pi$.

ii) Suppose that $h = \alpha_2$. Therefore the length sides of Q are common to two length sides of T (Figure 55-I).

Fig. 55. Planar representations.

One has $\alpha_1 + \delta < \alpha_1 + \gamma \le \pi$ (according to the Figure) and so $\alpha_2 > \gamma$. We may also verify that if $\beta \ge \alpha_1$, then the alternated angle sum around v cannot be defined. Therefore $\beta < \alpha_1$. And so

$$\alpha_1 + \gamma = \pi \qquad \text{and} \qquad \alpha_1 + k\delta = \pi, \quad \text{for some } k \ge 2. \qquad (3.5)$$

The PR is then extended as shown in Figure 55-II.

One gets a vertex w_1 surrounded by the cyclic sequence $(\alpha_2, \beta, \beta, \ldots)$. If valency of w_1 is bigger than four, then $\alpha_2 + \beta < \pi$. But if we add the smallest angle δ, it exceeds π (note that $\alpha_2 > \gamma$). Therefore w_1 has valency four, i.e., $\alpha_2 + \beta = \pi$.

If $\alpha_2 < \frac{\pi}{2}$, then $\beta + t\delta = \pi$ for some $t \ge 2$ (see the sequence of angles around v). Taking in account the length sides of Q and T, this alternated angle sum cannot be set up. Consequently $\alpha_2 = \frac{\pi}{2} = \beta$, and so $\alpha_2 + h = 2\alpha_2 = \pi$.

Fig. 56. Planar representation.

B)   Assume now that $z = \gamma$ (Figure 56).   Then $w \in \{\delta, \gamma\}$ and $h \in \{\delta, \beta, \alpha_2\}$.

Consider that $w = \delta$.   If $\alpha_1 + \delta = \pi$, then analyzing the length sides, we must have $\alpha_1 + \delta = \pi = \gamma + \delta$.   Consequently $\alpha_1 = \gamma$, leading us immediately to an absurd.

Suppose then that $\alpha_1 + \delta < \pi$.   With the labelling of Figure 57-I one has

$$x_1 = \alpha_2 \qquad \text{or} \qquad x_1 = \alpha_1 \qquad \text{or} \qquad x_1 = \delta.$$

Taking $x_1 = \alpha_2$, one gets two adjacent tiles (labelled by 2 and 3) such that the side of T opposite to γ is common to Q and α_1 and β are in adjacent positions.   By Proposition 3.1 (Page 14) there is not any dihedral f-tiling containing such adjacent tiles.

If $x_1 = \alpha_1$, then one gets two adjacent tiles (2 and 3) such that the side of T opposite to γ is common to Q and α_1 and δ are in adjacent positions.   As seen in A), γ and δ cannot be in adjacent positions, which is an absurd.

Now, one has $x_1 = \delta$, as illustrated in Figure 57-II, and it is clear that $x_{2i} = \gamma$ or $x_{2i} = \delta$ $(i \geq 1)$.

Fig. 57. Planar representations.

If $x_2 = \gamma$, then $\alpha_1 + \delta + \gamma \leq \pi$ and so $\beta > \alpha_1 > \frac{\pi}{2}$.   It follows that $\tilde{\theta} = \gamma$ or $\tilde{\theta} = \delta$.   The first situation leads to $\pi = \beta + \gamma = \alpha_2 + \beta > \pi$ (absurd), according to the length sides.   If $\tilde{\theta} = \delta$, then we must separate two distinct situations: 1) If α_1 and γ are in adjacent positions, then by Proposition 3.2 (Page 17), one has

$\beta = \frac{\pi}{2}$, which is not possible.   2) If α_1 and β are in adjacent positions, then by Proposition 3.1 there is not any f-tiling containing such tiles.   And so $x_2 = \delta$. A similar argumentation permit us to conclude that $x_{2i} = \delta$ $(i \geq 2)$.   Now, by using the length sides of the prototiles, we conclude that $x_{2i+1} = \delta$ $(i \geq 1)$. And therefore $x_i = \delta$ $(i \geq 1)$.   Consequently $\alpha_1 + k\delta = \pi = \gamma + k\delta$ for some $k \geq 2$.   This implies $\alpha_1 = \gamma < \beta$.   Using the labelling of Figure 57-II, we have no way to position another cells around u in order to fulfill the angle-folding relation.   And so $w = \gamma = z$.

Consider now that $h = \delta$ $(w = \gamma = z)$ (see Figure 58).
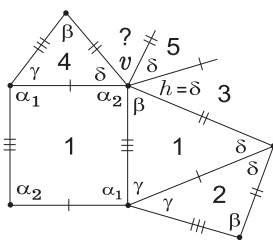
Fig. 58. Planar representation.

As $\alpha_2 + \delta < \alpha_1 + \gamma \leq \pi$, the valency of the vertex v is bigger than four and $\alpha_2 > \gamma$.   Consequently the alternated angle sum containing β must be $\beta + t\delta = \pi$ for some $t \geq 2$.   As α_1 and β cannot be adjacent angles (Proposition 3.1), the tile 4 is completely determined, as shown in refereed Figure.   However we have no way to avoid an incompatibility between sides.   And so $h = \beta$ or $h = \alpha_2$.

i) Suppose that $h = \beta$.   Then we achieve the *PR* below (Figure 59-I). On the other hand, $\alpha_1 + \gamma \leq \pi < \alpha_1 + \alpha_2$ and $\alpha_2 + \beta \leq \pi < \alpha_1 + \alpha_2$.   And so $\alpha_2 > \gamma$ and $\alpha_1 > \beta$.   Therefore $\alpha_1 + \gamma = \pi$ and $\alpha_2 + h = \alpha_2 + \beta = \pi$.

ii) Suppose that $h = \alpha_2$ (Figure 59-II).   This situation is precisely the one considered in Figure 55-I (Page 34), in case A) ii).   Consequently, as before, we must have $\alpha_2 = \beta = \frac{\pi}{2}$.   And so $\alpha_2 + h = 2\alpha_2 = \pi$.   □
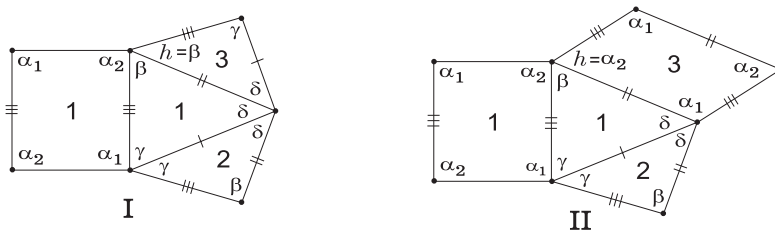
Fig. 59. Planar representations.

PROPOSITION 3.7.   *With the terminology used in Figure 51 (Page 32),*
i)   *if $h = \alpha_2$, then $\tau = \mathcal{T}^k$, $k \geq 2$;*
ii) *if $h = \beta$ and $z = \delta$, then $\tau = \mathcal{M}$ or $\tau = \mathcal{R}^k_{\beta\delta}$, $k \geq 2$;*
iii) *if $h = \beta$ and $z = \gamma$, then $\tau = \mathcal{T}^k$, $k \geq 2$ or $\tau = \mathcal{R}^k_{\beta\gamma}$, $k \geq 3$,*
where the internal angles of the prototiles are given by:

$$\alpha_1 = \frac{(k+1)\pi}{2k+1} \quad \alpha_2 = \frac{\pi}{2} \quad \beta = \frac{\pi}{2} \quad \gamma = \frac{k\pi}{2k+1} \quad \delta = \frac{\pi}{2k+1} \quad \text{in } \mathcal{T}^k, k \geq 2;$$

$$\alpha_1 = \frac{3\pi}{5} \qquad \alpha_2 = \frac{\pi}{2} \quad \beta = \frac{\pi}{2} \quad \gamma = \frac{\pi}{3} \qquad \delta = \frac{\pi}{5} \qquad \text{in } \mathcal{M}.$$

For $\mathcal{R}^k_{**}$ the following relations take place:
- *In $\mathcal{R}^2_{\beta\delta}$, one has $\alpha_1 + \delta = \pi$, $\alpha_2 + \beta = \pi$ and $\gamma = \frac{\pi}{2}$. The angles β and δ verify $\cos\beta = \frac{\sqrt{2}}{2}\left(\sin\frac{\theta}{2} - \cos\frac{\theta}{2}\sin x\right)$ and $\cos\delta = \frac{\sqrt{2}}{2}\left(\sin\frac{\theta}{2} + \cos\frac{\theta}{2}\sin x\right)$ for some $x \in \left]0, \frac{\pi}{2}\right[$ and $\theta \in \left]0, 2\arctan(\sin x)\right[$.   In particular, $0 < \delta < \frac{\pi}{2} < \beta < \frac{3\pi}{4}$.*
- *In $\mathcal{R}^k_{\beta\delta}$, $k \geq 3$, one has $\alpha_1 + \delta = \pi$, $\alpha_2 + \beta = \pi$ and $\gamma = \frac{\pi}{k}$; where $\cos\beta = \sin\frac{\pi}{2k}\sin\frac{\theta}{2} - \cos\frac{\pi}{2k}\cos\frac{\theta}{2}\sin x$ and $\cos\delta = \sin\frac{\pi}{2k}\sin\frac{\theta}{2} + \cos\frac{\pi}{2k}\cos\frac{\theta}{2}\sin x$ for some $(x,\theta) \in R_k$ (R_k is the region of $\left]0,\frac{\pi}{2}\right[\times \left]0,\pi\right[$ represented in Figure 73 (Page 45) and Figure 74). Here $\pi - \frac{2\pi}{k} < \beta < \pi - \frac{\pi}{2k}$, $0 < \delta < \frac{\pi}{k}$.*
- *In $\mathcal{R}^k_{\beta\gamma}$, $k \geq 3$, one has $\alpha_1 + \gamma = \pi$, $\alpha_2 + \beta = \pi$ and $\delta = \frac{\pi}{k}$. The angles β and γ obey $\cos\beta = \sin\frac{\pi}{2k}\sin\frac{\theta}{2} - \cos\frac{\pi}{2k}\cos\frac{\theta}{2}\sin x$ and $\cos\gamma = \sin\frac{\pi}{2k}\sin\frac{\theta}{2} + \cos\frac{\pi}{2k}\cos\frac{\theta}{2}\sin x$ for some $(x,\theta) \in R'_k$ (the region R'_k is represented in Figure 77 (Page 48) and Figure 78). Here $\frac{\pi}{2} - \frac{\pi}{2k} < \beta < \pi - \frac{\pi}{k}$, $\frac{\pi}{k} < \gamma < \frac{\pi}{2}$.*

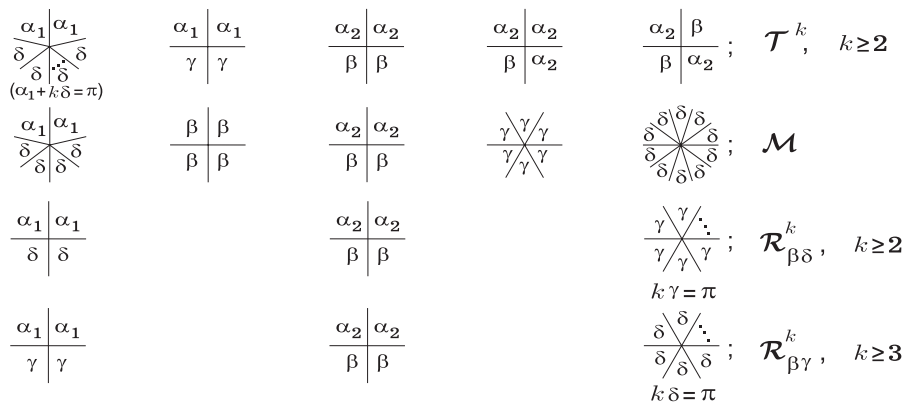*The angles around vertices are represented in Figure 60.*

Fig. 60.   Distinct classes of congruent vertices.

Figure 64 *(Page* 39*) illustrates* 3D *representations of* $\mathscr{T}^k$ *for* $k = 3$ *and* $k = 4$. *Figure* 69-III *(Page* 42*) illustrates a* 3D *representation of* $\mathscr{M}$. *Figure* 71 *(Page* 43*) illustrates a* 3D *representation of* $\mathscr{R}^2_{\beta\delta}$. *Figure* 75 *(Page* 46*) illustrates* 3D *representations of* $\mathscr{R}^k_{\beta\delta}$ *for* $k = 3$ *and* $k = 4$. *Figure* 79 *(Page* 49*) illustrates* 3D *representations of* $\mathscr{R}^k_{\beta\gamma}$ *for* $k = 3$ *and* $k = 4$.

PROOF. i) Suppose that $h = \alpha_2$. Then, as seen in Proposition 3.6 A) ii) and B) ii), one gets the *PR* illustrated in Figure 55-II (Page 34), where $\alpha_1 + \gamma = \pi$, $\alpha_1 + k\delta = \pi$ $(k \geq 2)$ and $\alpha_2 = \frac{\pi}{2} = \beta$.

If the cyclic sequence of angles around w_1 (Figure 55-II) is $(\alpha_2, \beta, \beta, \beta)$, then one gets a vertex enclosed by at least three angles γ in adjacent positions. And, in order to obey the angle-folding relation we must have $3\gamma = \pi$ (note that the cyclic sequence $(\gamma, \gamma, \gamma, \delta, \delta, \gamma)$ with $2\gamma + \delta = \pi$ may not occur, since it leads us to a vertex surrounded by $(\alpha_1, \delta, \gamma, \ldots)$, where the angle-folding relation will fail). It follows by (3.5) (Page 34) that $\gamma + \delta = \frac{\pi}{3} + \frac{\pi}{3k} \leq \frac{\pi}{2}$, which is not possible. Thus the cyclic sequence of angles around w must be $(\alpha_2, \beta, \beta, \alpha_2)$ $(\alpha_2 + \beta = \pi)$.

The *PR* illustrated in Figure 55-II is now extended as seen in Figure 61-I (for $k = 2$) or Figure 61-II (for $k = 3$). The case $k \geq 4$ is similar.
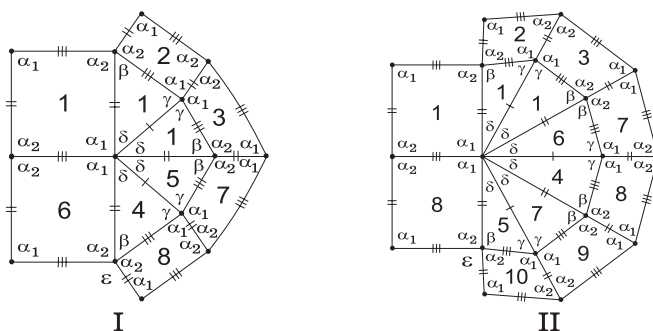
Fig. 61. Planar representations.

With the labelling of Figure 61, we have $\varepsilon \in \{\alpha_2, \beta\}$. It can be shown that either $\varepsilon = \beta$ or $\varepsilon = \alpha_2$ lead to the same configuration. Considering for instance $\varepsilon = \beta$, a complete *PR* is uniquely achieved. In Figure 62 a complete *PR* of such an f-tiling is presented. We consider $k = 2$ for commodity.

Bisecting Q through α_1, one gets two congruent triangles T_1 and T_2 (see Figure 63). The triangles T, T_1 and T_2 have a common angle $\alpha_2 = \beta$ and two congruent sides. Hence they are congruent triangles. And so $x_0 = \gamma$ and $y_0 = \delta$. This information shows that $\alpha_1 = \gamma + \delta$. By (3.5) (Page 34) we conclude that
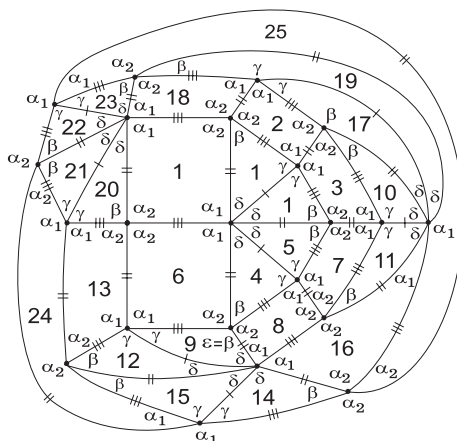
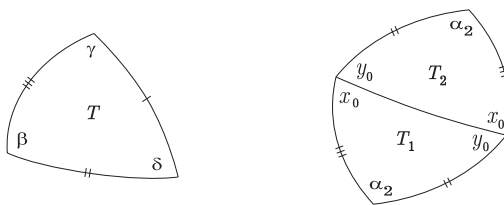**Fig. 62.** Extended planar representation of $\mathcal{T}^2$.

Fig. 63. Decomposition of Q.

$$\delta = \frac{\pi}{2k+1}, \quad \gamma = \frac{k\pi}{2k+1} \quad \text{and} \quad \alpha_1 = \frac{(k+1)\pi}{2k+1}, \qquad k \geq 2.$$

Such a family of dihedral f-tilings is denoted by $\mathcal{T}^k$, $k \geq 2$ (composed of $8k$ triangles and $4(k+1)$ quadrangles). In Figure 64 3D representations of $\mathcal{T}^2$ and $\mathcal{T}^3$ are illustrated, respectively.

Bisecting all congruent quadrangles of $\mathcal{T}^k$ by α_1 ($k \geq 2$), one gets a monohedral f-tiling established in [4] and [11]. The prototile-triangle has internal angles $\frac{\pi}{2}$, $\frac{k\pi}{2k+1}$ and $\frac{\pi}{2k+1}$. This justify the compatibility between angles and sides of $\mathcal{T}^k$.

ii) Suppose that $h = \beta$ and $z = \delta$. By Proposition 3.6 the tiles labelled by 1 and 2 (Figure 65-I and Figure 65-II) are uniquely determined. Besides, $\alpha_2 + \beta = \pi$. (In fact, the inequality $\alpha_2 + \beta < \pi$ leads us to a contradiction, as seen in case A)i) of the proof of Proposition 3.6). Now, one gets necessarily one of the *PRs* illustrated in Figure 65 (by using the length sides and the relation $\alpha_1 > \alpha_2 > \delta$). As $\alpha_1 + \delta \leq \pi$ and $\alpha_1 > \beta$ (note that $\alpha_1 + \alpha_2 > \pi = \alpha_2 + \beta$), we have $\alpha_1 + k\delta = \pi$ for some $k \geq 1$.
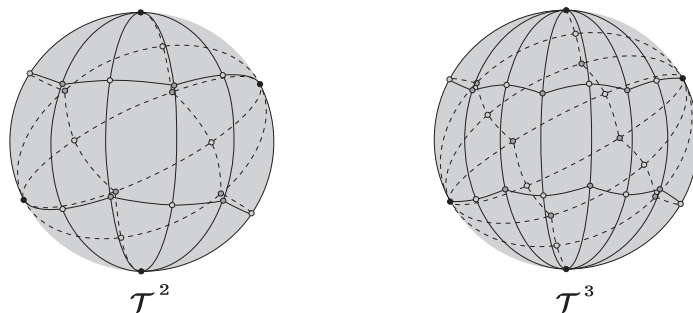
Fig. 64. 3D representations.
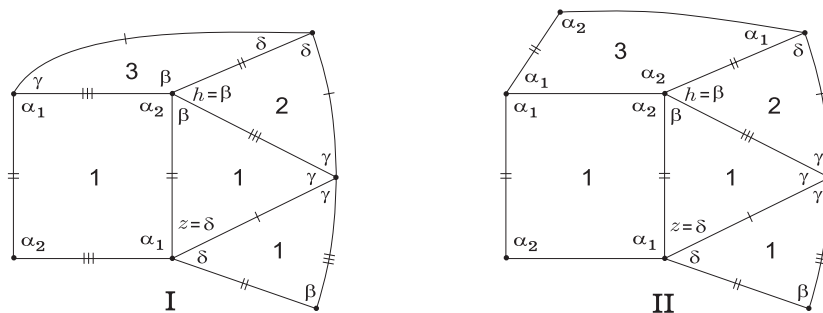
Fig. 65. Planar representations.

(1) Suppose firstly that $\alpha_1 + \delta < \pi$ (i.e., $\alpha_1 + k\delta = \pi$, $k \geq 2$).

(1.1) If the tile 3 is a triangle (Figure 65-I), then one gets in a unique way the *PR* illustrated in Figure 66, achieving $\alpha_1 + \gamma = \pi$, $\alpha_2 = \frac{\pi}{2} = \beta$, $2\gamma + \delta = \pi$ and $\gamma + (k+1)\delta = \pi$ for some $k \geq 2$ (hence $\alpha_1 = \frac{(k+1)\pi}{2k+1}$, $\gamma = \frac{k\pi}{2k+1}$ and $\delta = \frac{\pi}{2k+1}$). In Figure we took $k = 2$ for commodity.

Note: On the construction of the *PR* illustrated in Figure 66, we recall that: a) If we replace γ by δ in triangle 7, we get an incompatibility between sides around such vertex. b) On the other hand if we replace δ by γ in the tile 8, then $\gamma = \frac{\pi}{3}$ (note that $2\gamma + 2\delta > \pi$), and we have $k\delta = \frac{\pi}{3}$ for some $k \geq 2$ (because $\alpha_1 + \gamma = \pi = \alpha_1 + k\delta$). It follows that $\beta + \gamma + \delta \leq \frac{\pi}{2} + \frac{\pi}{3} + \frac{\pi}{6} = \pi$, which is absurd. c) Taking in account the length sides and considering that the cyclic sequence $(\gamma, \delta, \alpha_1, \ldots)$ may not occur, it follows that the tile 15 is also completely determined. At the final step, one gets a vertex surrounded by the sequence $(\gamma, \gamma, \gamma, \gamma, \gamma, \ldots)$, leading us to an absurd, since $3\gamma > 2\gamma + \delta = \pi$.

(1.2) Suppose now that the tile 3 is a quadrangle (Figure 65-II). We shall discern the cases $\gamma = \frac{\pi}{2}$ and $\gamma < \frac{\pi}{2}$.
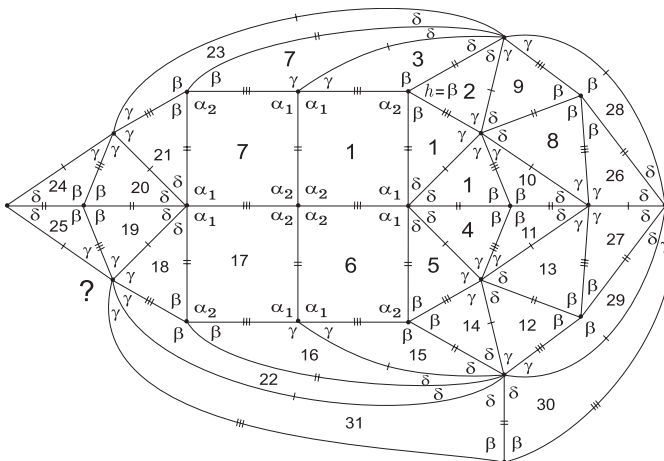
Fig. 66.   Planar representation.

If $\gamma = \frac{\pi}{2}$, then $\beta > \frac{\pi}{2} > \alpha_2$. Hence the *PR* illustrated in Figure 65-II is extended as shown in Figure 67-I. However, there is no way to avoid a vertex surrounded by the cyclic sequence of angles $(\beta, \alpha_2, \gamma, \ldots)$, where the angle-folding relation is violated, since $\beta + \gamma > 2\gamma = \pi$.
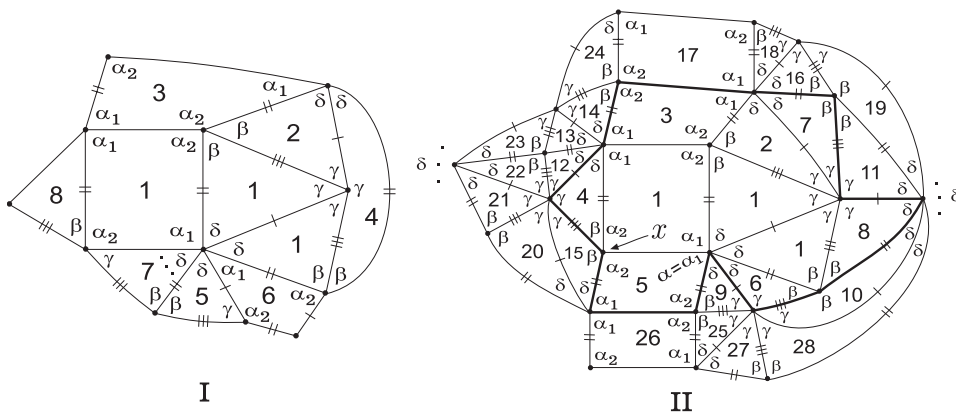

Fig. 67.   Planar representations.

Let now $\gamma < \frac{\pi}{2}$. Starting from the *PR* represented in Figure 65-II and taking in account that $\alpha_1 + k\delta = \pi$ for some $k \geq 2$, we get in a unique way the *PR* composed by tiles labelled from 1 to 8 (contained in Figure 67-II). The crucial step here is to prove that the angle α in the tile 5 must be α_1. In fact,

we have clearly $\alpha \neq \alpha_2$, and by Proposition 3.1 (Page 14) we also have $\alpha \neq \beta$. An argument using length sides shows that α cannot be δ. Finally, if $\alpha = \gamma$, then the cyclic sequence of angles $(\beta, \alpha_2, \beta, \ldots)$ around the vertex x must take place. Since the cyclic sequence $(\beta, \alpha_2, \beta, \beta)$ cannot occur (otherwise a partial tiling in Figure 65-I appears, which we already show the incompatibility), it follows that x has to be surrounded by $(\beta, \alpha_2, \beta, \alpha_2)$, and consequently there must be a vertex surrounded by $(\alpha_1, \delta, \gamma, \ldots)$, where the angle folding relation fails. And hence $\alpha = \alpha_1$. One has, $\alpha_2 = \beta = \frac{\pi}{2}$ and $3\gamma \leq \pi$. Consequently $\gamma + \delta > \frac{\pi}{2}$. As δ is the least angle, we have $3\gamma = \pi$, i.e., $\gamma = \frac{\pi}{3}$. Now, if $k \geq 3$, then $\delta < \frac{\pi}{6}$ (because $\alpha_1 > \frac{\pi}{2}$). And so $\beta + \gamma + \delta < \frac{\pi}{2} + \frac{\pi}{3} + \frac{\pi}{6} = \pi$, which is an absurd. Therefore $k = 2$ and $\frac{\pi}{6} < \delta < \frac{\pi}{4}$. The tiles labelled from 9 to 28 (Figure 67-II) come in a unique way. And this PR is extended until it "closes" (Figure 68). Such an extension is unique and leads us to conclude that $\delta = \frac{\pi}{5}$ since $\frac{\pi}{6} < \delta < \frac{\pi}{4}$. The angles of Q and T are completely determined and given by

$$\alpha_1 = \frac{3\pi}{5}, \qquad \alpha_2 = \frac{\pi}{2} = \beta, \qquad \gamma = \frac{\pi}{3} \qquad \text{and} \qquad \delta = \frac{\pi}{5}.$$
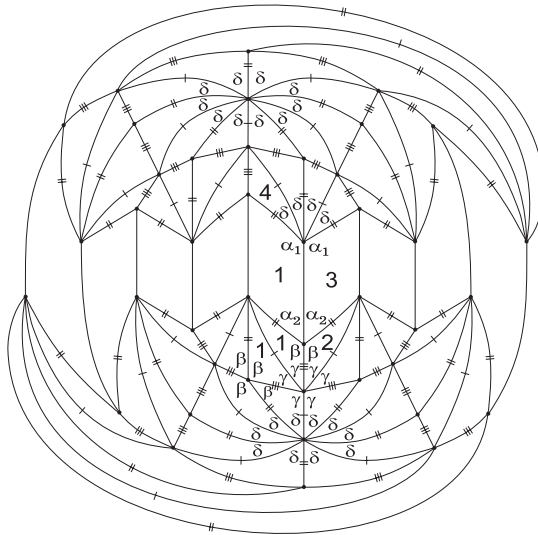

Fig. 68. Planar representation.

The previous extended PR was obtained from an extended PR of $\mathcal{G}_3$ (studied in [3]), deleting one pair of opposite sides of Q (compare Figure 69-II with Figure 69-III) and preserving the angle-folding relation. We shall denote such an f-tiling by $\mathcal{M}$. Its 3D representation is shown in Figure 69-III,

composed of 60 triangles and 10 quadrangles. (Note: Bisecting by α_1 and by α_2 any quadrangle of $\mathcal{G}_3$, one gets a monohedral (f-)tiling (Figure 69-I), [4], [11].)
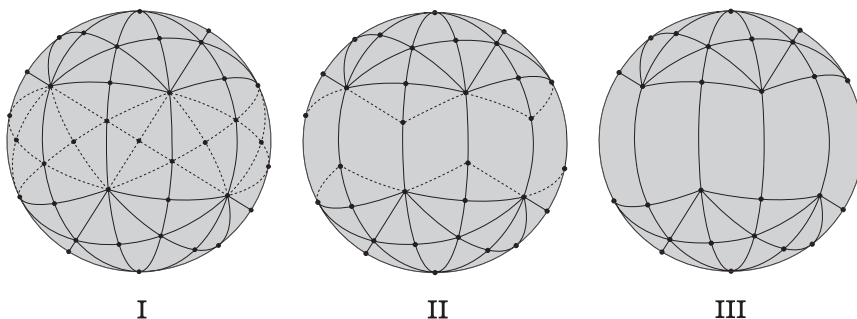

Fig. 69. 3D representations of a monohedral tiling $\mathcal{G}_3$ and $\mathcal{M}$, respectively.

(2)   Assume now that $\alpha_1 + \delta = \pi$.

(2.1)   If the tile 3 is a triangle (Figure 65-I, Page 40), then one gets α_1 and γ in adjacent positions, where the angle-folding relation fails. (Note that the alternated angle sum containing α_1 must be $\alpha_1 + \delta = \pi$. But, this leads to an incompatibility between sides.)

(2.2)   Suppose now that the tile 3 is a quadrangle (Figure 65-II). The extension of the PR leads to $\gamma = \frac{\pi}{k}$ for some $k \geq 2$. Any extended PR is composed of $2k$ spherical moons with vertices surrounded by γ. Such f-tilings are denoted by $\mathcal{R}_{\beta\delta}^{k}$. Each spherical moon has two congruent triangles and one quadrangle at its center. In Figure 70 a complete PR for $k = 2$ is illustrated.

(2.2.1)   Consider firstly that $\gamma = \frac{\pi}{2}$. In this case the PR is the same as the one illustrated in Figure 48 (Page 30), permuting β with γ.
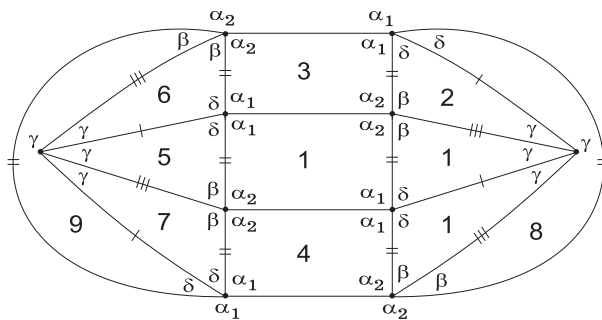

Fig. 70. Planar representation.

With the terminology and notation used in the proof of Proposition 3.5 ii) (Page 28), one has

$$\cos \beta = \frac{\sqrt{2}}{2}\left(\sin\frac{\theta}{2} - \cos\frac{\theta}{2}\sin x\right) \qquad \text{and} \qquad \cos\delta = \frac{\sqrt{2}}{2}\left(\sin\frac{\theta}{2} + \cos\frac{\theta}{2}\sin x\right).$$

And we have (Figure 50, Page 31)

- $\forall x \in \left]0,\frac{\pi}{2}\right[, \quad \forall\theta \in \left]0, 2\arctan(\sin x)\right[, \qquad \frac{\pi}{2} < \beta < \frac{3\pi}{4};$

- $\forall x \in \left]0,\frac{\pi}{2}\right[, \quad \forall\theta \in \left]0, 2\arctan(\sin x)\right[, \qquad 0 < \delta < \frac{\pi}{2}.$

In Figure 71 a 3D representation of $\mathscr{R}^2_{\beta\delta}$ is illustrated.
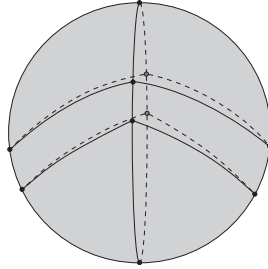
Fig. 71. 3D representation.

Note that (Figure 50, Page 31) if $\theta = 0$ and $0 < x < \frac{\pi}{2}$, then one gets a family of monohedral f-tilings [4], [11]. The prototile is a spherical triangle T with internal angles $\frac{\pi}{2}$, β and δ such that $\beta + \delta = \pi$ and $\frac{\pi}{4} < \delta < \beta < \frac{3\pi}{4}$.

(2.2.2) Suppose that $\gamma = \frac{\pi}{k}$ for some $k \geq 3$. The quadrangle Q is congruent to a WCSQ* $L_1 \cap L_2$, where L_1 and L_2 are two non-orthogonal well centered spherical moons with distinct angle measure θ and θ_1 $(\theta \neq \theta_1)$, respectively. Similar to Proposition 3.5 ii) (Page 28) we may suppose that $\theta_1 = \gamma = \frac{\pi}{k}$ for some $k \geq 3$ and $0 < \theta < \pi$, $\theta \neq \frac{\pi}{k}$ (Figure 72).

With the labelling of this Figure 72, one gets

$$\cos\delta = \sin\frac{\pi}{2k}\sin\frac{\theta}{2} + \cos\frac{\pi}{2k}\cos\frac{\theta}{2}\sin x \qquad (3.6)$$

and

$$\cos\beta = \sin\frac{\pi}{2k}\sin\frac{\theta}{2} - \cos\frac{\pi}{2k}\cos\frac{\theta}{2}\sin x,$$

for some $x \in \left]0,\frac{\pi}{2}\right[$ $\left(x = \frac{\pi}{2} - \measuredangle(L_1, L_2)\right)$ and $\theta \in \left]0,\pi\right[$, $\theta \neq \frac{\pi}{k}$, $k \geq 3$.
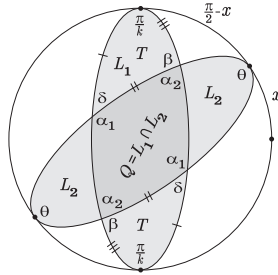
Fig. 72. A WCSQ.

For any x, x_1, x_2, $x_1 < x_2$ and θ, θ_1, θ_2, $\theta_1 < \theta_2$ such that $x \in \left]0, \frac{\pi}{2}\right[$, $x_i \in \left]0, \frac{\pi}{2}\right[$ and $\theta \in]0, \pi[$, $\theta_i \in]0, \pi[$, $i = 1, 2$, one has

$$\beta(x, \theta_1) > \beta(x, \theta_2), \qquad \beta(x_1, \theta) < \beta(x_2, \theta) \qquad \text{and} \qquad \delta(x_1, \theta) > \delta(x_2, \theta).$$

Extending the functions δ and β to $\left[0, \frac{\pi}{2}\right] \times [0, \pi]$ it follows that

$$\beta(x, \theta) \leq \beta(x, 0) \leq \beta\left(\frac{\pi}{2}, 0\right) = \pi - \frac{\pi}{2k}$$

and

$$\delta(x, \theta) \geq \delta\left(\frac{\pi}{2}, \theta\right) = \left|\frac{\pi}{2k} - \frac{\theta}{2}\right| \geq \delta\left(\frac{\pi}{2}, \frac{\pi}{k}\right) = 0,$$

for all $x \in \left[0, \frac{\pi}{2}\right]$ and $\theta \in [0, \pi]$. This inequality implies $\theta < \frac{3\pi}{k}$, since $\delta < \frac{\pi}{k}$.

Now, for each $k \geq 3$ we must determine a region $R_k \subset \left]0, \frac{\pi}{2}\right[\times]0, \pi[$ such that

$$\delta = \delta(x, \theta) < \frac{\pi}{k} = \gamma \qquad \text{iff} \quad (x, \theta) \in R_k.$$

By (3.6),

$$\delta < \frac{\pi}{k} \Leftrightarrow \cos \delta > \cos \frac{\pi}{k} \Leftrightarrow x > \arcsin \frac{\cos \frac{\pi}{k} - \sin \frac{\pi}{2k} \sin \frac{\theta}{2}}{\cos \frac{\pi}{2k} \cos \frac{\theta}{2}} = x_k(\theta), \quad 0 < \theta < \frac{3\pi}{k}.$$

Observe that, for any $k \geq 3$, $x_k(0) = \arcsin \frac{\cos \frac{\pi}{k}}{\cos \frac{\pi}{2k}}$. Besides, $x_k\left(\frac{3\pi}{k}\right) = \frac{\pi}{2}$, if $k \geq 4$, and $x_3(\pi) = 0$.

For any $k \geq 3$, one has
- $\delta < \frac{\pi}{k}$ iff $x > x_k(\theta)$;
- $\delta = \frac{\pi}{k}$ iff $x = x_k(\theta)$;
- $\delta > \frac{\pi}{k}$ iff $x < x_k(\theta)$ or $\frac{3\pi}{k} < \theta < \pi$ (in case $k \geq 4$).

The region R_k is then

$$R_k = \left\{ (x,\theta) \in \left]0,\frac{\pi}{2}\right[\times \left]0,\pi\right[: 0 < \theta < \frac{3\pi}{k}, \theta \neq \frac{\pi}{k} \text{ and } x_k(\theta) < x < \frac{\pi}{2}\right\}. \quad (3.7)$$

In Figure 73 we represent graphically R_k $(k \geq 4)$. (The case $k = 3$ is somewhat different—the dash line $x = x_k(\theta)$ joins the points $\left(\arcsin\frac{1}{\sqrt{3}}, 0\right)$ and $(0,\pi)$, Figure 74.) The case $\theta = \frac{\pi}{k}$ is excluded.
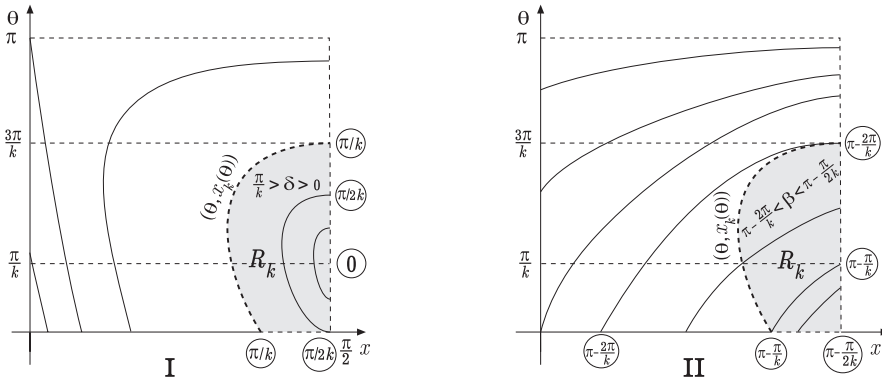

Fig. 73. Contour levels of δ and β $(k \geq 4)$.

For all $(x,\theta) \in R_k$ and $k \geq 3$ one gets

$$\gamma = \frac{\pi}{k} \leq \pi - \frac{2\pi}{k} = \beta\left(\frac{\pi}{2}, \frac{3\pi}{k}\right) < \beta = \beta(x,\theta) < \beta\left(\frac{\pi}{2}, 0\right) = \pi - \frac{\pi}{2k}.$$

The contour levels of δ and β are illustrated in Figure 73-I and Figure 73-II, respectively (if $k = 3$, see Figure 74-I and Figure 74-II). The value of contour level is signalized into a circle.

Limit cases: Note that

1. If $x = x_k(\theta)$, $0 < \theta < \frac{3\pi}{k}$, $\theta \neq \frac{\pi}{k}$, then $\delta = \gamma = \frac{\pi}{k}$, giving rise to a family of dihedral f-tilings established in Proposition 2.2 (Page 6). In addition if $\theta = \frac{\pi}{k}$, then Q has all congruent sides and $\beta = \arccos\left(1 - 2\cos\frac{\pi}{k}\right) = 2\arccos\sqrt{1 - \cos\frac{\pi}{k}}$ (see [3]);

2. If $\theta = 0$ and $\arcsin\frac{\cos\frac{\pi}{k}}{\cos\frac{\pi}{2k}} \leq x < \frac{\pi}{2}$, then one gets a family of monohedral f-tilings (see [4], [11]). The prototile has internal angles $\frac{\pi}{k}$, δ and β such that $\delta + \beta = \pi$ and $\frac{\pi}{2k} < \delta \leq \frac{\pi}{k}$, $\pi - \frac{\pi}{k} \leq \beta < \pi - \frac{\pi}{2k}$.

Figure 75 illustrates 3D representations of $\mathscr{R}_{\beta\delta}^k$ for $k = 3$ and $k = 4$.

iii)   Finally we shall suppose that $h = \beta$ and $z = \gamma$. One has $\alpha_1 + \gamma = \pi$ and $\alpha_2 + \beta = \pi$, as seen in Proposition 3.6 B) i) (Figure 59-I, Page 36). We
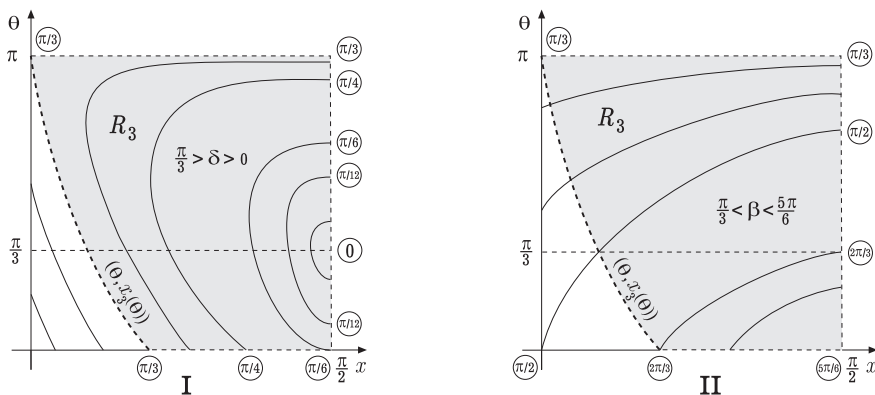
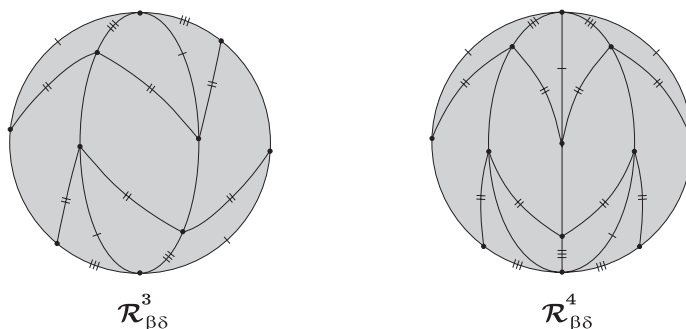**Fig. 74.** Contour levels of δ and β $(k = 3)$.

Fig. 75. 3D representations.

shall consider two cases when the tile 5 (Figure 76) is a triangle or a quadrangle.

(1) Suppose firstly that the tile 5 is a triangle. Then it has to be set up as illustrated in Figure 76-I. Now, as we have a quadrangle (labelled 1) and a triangle (labelled 5) in adjacent positions such that α_1 and δ are adjacent angles as well as α_2 and β, we must have $\varepsilon_1 = \delta$ by Proposition 3.6 A) (Page 32), and with the labelling of Figure 76-I. One gets $\alpha_1 + \delta < \alpha_1 + \gamma = \pi$. Now, as seen in case ii) (Figure 65-I, Page 40) this PR cannot be contained in a complete PR of any element of $\Omega(Q, T)$.

(2) If the tile 5 is a quadrangle, then one gets the PR illustrated in Figure 76-II. With the labelling of this Figure, one has $\varepsilon_2 = \alpha_2$ or $\varepsilon_2 = \beta$.

The first case leads in a unique way to get an extended PR of $\mathscr{T}^k$ (Figure 64 in Page 39), where $\alpha_1 + k\delta = \pi$ for some $k \geq 2$ (obtained in case i)).
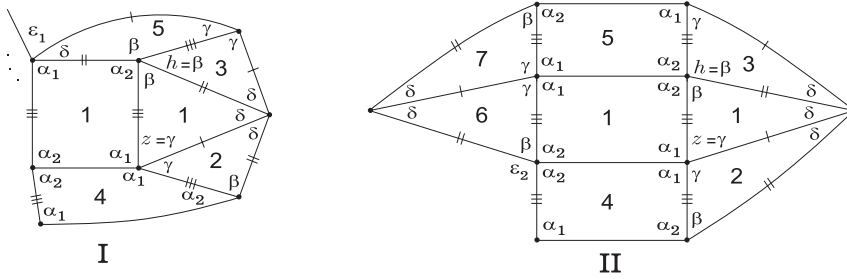
Fig. 76. Planar representations.

We should then consider $\varepsilon_2 = \beta$ and an extended PR is composed of $2k$ $(k \geq 3)$ spherical moons (with two congruent triangles and one quadrangle at its center), where $\delta = \frac{\pi}{k}$, $\alpha_1 + \gamma = \pi$ and $\alpha_2 + \beta = \pi$. Such f-tilings are denoted by $\mathscr{R}^k_{\beta\gamma}$.

With a similar procedure taken in case ii) (see (3.6), Page 44), for each $k \geq 3$ one has

$$\cos \gamma = \sin \frac{\pi}{2k} \sin \frac{\theta}{2} + \cos \frac{\pi}{2k} \cos \frac{\theta}{2} \sin x$$

and

$$\cos \beta = \sin \frac{\pi}{2k} \sin \frac{\theta}{2} - \cos \frac{\pi}{2k} \cos \frac{\theta}{2} \sin x,$$

for some $x \in \left]0, \frac{\pi}{2}\right[$ and $\theta \in \left]0, \pi\right[$, $\theta \neq \frac{\pi}{k}$.

The set $R'_k \subset \left]0, \frac{\pi}{2}\right[\times \left]0, \pi\right[$ such that

$$\gamma = \gamma(x, \theta) > \frac{\pi}{k} = \delta \qquad \text{iff} \quad (x, \theta) \in R'_k$$

is given by the condition

$$R_k \;\dot\cup\; R'_k \;\dot\cup\; C_k = \left]0, \frac{\pi}{2}\right[\times \left]0, \pi\right[\setminus \left\{ \frac{\pi}{k} \right\},$$

where R_k is the set described in case ii) (see (3.7), Page 45) and

$$C_k = \left\{ (x, \theta) \in \left]0, \frac{\pi}{2}\right[\times \left]0, \pi\right[: \gamma(x, \theta) = \delta = \frac{\pi}{k}, \theta \neq \frac{\pi}{k} \right\}.$$

The dark zone of Figure 77 is the set R'_k $(k \geq 4)$. As before the case $k = 3$ has to be considered separately (Figure 78). The line $\theta = \frac{\pi}{k}$ is excluded. For all $(x, \theta) \in R'_k$ $(k \geq 3)$ one gets $\frac{\pi}{k} < \gamma(x, \theta) < \frac{\pi}{2}$ and $\frac{\pi}{2} - \frac{\pi}{2k} < \beta(x, \theta) < \pi - \frac{\pi}{k}$.

In Figure 77-I and Figure 77-II the contour levels of γ and β are illustrated, respectively (for the case $k = 3$, see Figure 78-I and Figure 78-II). Note that if $k = 3$, then $\frac{\pi}{2} - \frac{\pi}{2k} = \pi - \frac{2\pi}{k} = \frac{\pi}{3}$.
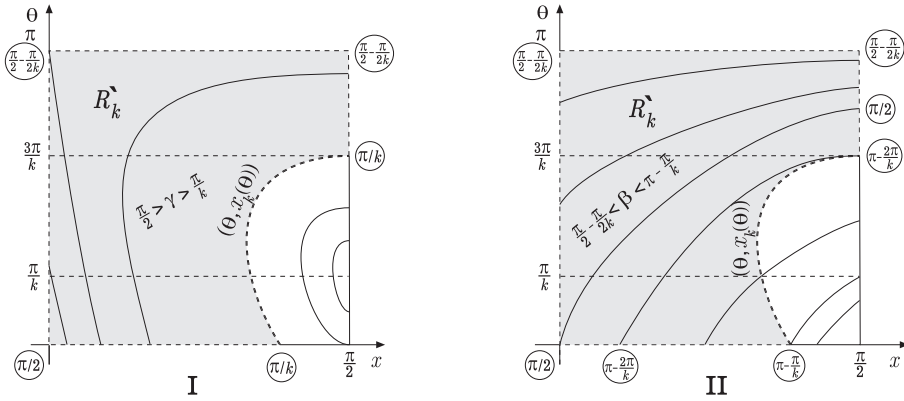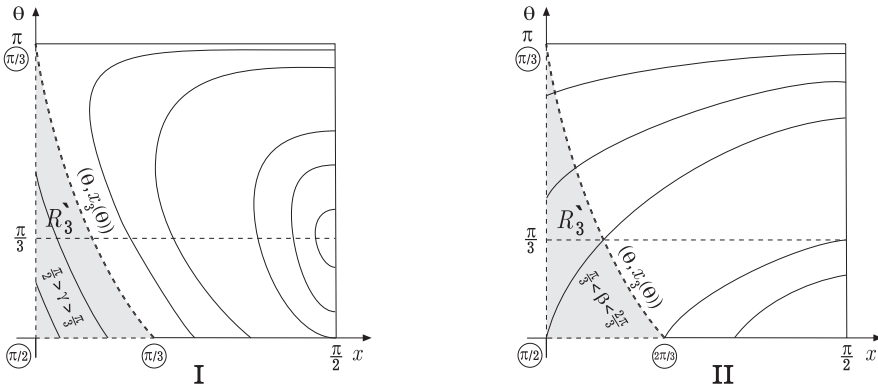

Fig. 77. Contour levels of γ and β $(k \geq 4)$.

Fig. 78. Contour levels of γ and β $(k = 3)$.

Figure 79 illustrates 3D representations of $\mathscr{R}^k_{\beta\gamma}$ for $k = 3$ and $k = 4$.

$\square$

In Table 1 it is shown a complete list of all dihedral f-tilings, whose prototiles are a scalene spherical triangle of angles β, γ, δ with $\beta > \gamma > \delta$ and a WCSQ* (a spherical quadrangle with distinct pairs of congruent opposite sides and distinct pairs of congruent opposite angles say α_1, α_2, $\alpha_1 > \alpha_2$). We have used the following notation.
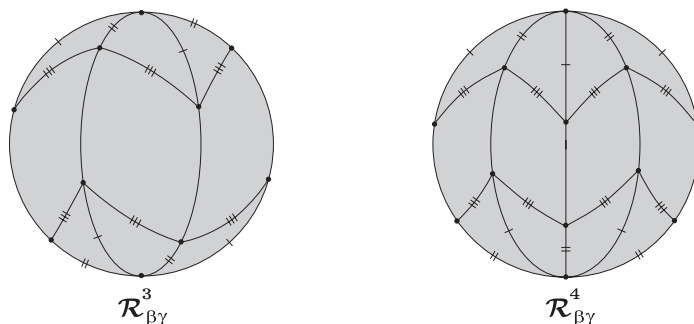
$$\mathcal{R}_{\beta\gamma}^{3} \qquad\qquad \mathcal{R}_{\beta\gamma}^{4}$$

Fig. 79. 3D representations.

f-tiling	α_1	α_2	β	γ	δ	$|V|$	M	N
$\mathscr{R}_{\gamma\delta}^{2}$	$\pi - \delta$	$\pi - \gamma$	$\frac{\pi}{2}$	$]\frac{\pi}{4}, \frac{\pi}{2}[$	$]0, \frac{\pi}{2}[$	3	4	8
$\mathscr{R}_{\beta\delta}^{2}$	$\pi - \delta$	$\pi - \beta$	$]\frac{\pi}{2}, \frac{3\pi}{4}[$	$\frac{\pi}{2}$	$]0, \frac{\pi}{2}[$	3	4	8
$\mathscr{R}_{\beta\delta}^{k}, \ k \geq 3$	$\pi - \delta$	$\pi - \beta$	$]b_k, d_k[$	$\frac{\pi}{k}$	$]0, \frac{\pi}{k}[$	3	$2k$	$4k$
$\mathscr{R}_{\beta\gamma}^{k}, \ k \geq 3$	$\pi - \gamma$	$\pi - \beta$	$]a_k, c_k[$	$]\frac{\pi}{k}, \frac{\pi}{2}[$	$\frac{\pi}{k}$	3	$2k$	$4k$
$\mathscr{M}_{\alpha_2}^{3}$	$\frac{2\pi}{3}$	$]\frac{\pi}{3}, \frac{2\pi}{3}[\backslash\{\frac{\pi}{2}\}$	$\frac{\pi}{2}$	$\frac{\pi}{3}$	$\frac{\pi - \alpha_2}{2}$	4	6	24
$\mathscr{M}_{\alpha_2}^{k}, \ k \geq 4$	$\frac{(k-1)\pi}{k}$	$]\frac{\pi}{k}, \frac{2\pi}{k}[\backslash\{\alpha_2^k\}$	$\frac{\pi}{2}$	$\frac{\pi - \alpha_2}{2}$	$\frac{\pi}{k}$	4	$2k$	$8k$
$\mathscr{T}^{k}, \ k \geq 2$	$\frac{(k+1)\pi}{2k+1}$	$\frac{\pi}{2}$	$\frac{\pi}{2}$	$\frac{k\pi}{2k+1}$	$\frac{\pi}{2k+1}$	5	$4k+4$	$8k$
$\mathscr{M}$	$\frac{3\pi}{5}$	$\frac{\pi}{2}$	$\frac{\pi}{2}$	$\frac{\pi}{3}$	$\frac{\pi}{5}$	5	10	60

Table 1.   Dihedral f-Tilings by Scalene Triangles and WCSQ*

- $a_k = \frac{\pi}{2} - \frac{\pi}{2k}$, $b_k = \pi - \frac{2\pi}{k}$, $c_k = \pi - \frac{\pi}{k}$ and $d_k = \pi - \frac{\pi}{2k}$;
- $\alpha_2^k = \arccos\left(2\cos\frac{\pi}{k} - 1\right)$;
- The f-tilings $\mathscr{R}_{\phi_1\phi_2}^{k}$ $(k \geq 2)$ obey $\cos\phi_1 + \cos\phi_2 = 2\sin\frac{\pi}{2k}\sin\frac{\theta}{2}$ for some θ;
- $|V|$ is the number of distinct classes of congruent vertices;
- N and M are the number of triangles congruent to T and the number of quadrangles congruent to Q, respectively used in such dihedral f-tilings.

In Figure 80 we present a complete list of all dihedral f-tilings, whose prototiles are a spherical triangle T and a WCSQ Q. A detailed study of the f-tilings is included in [2] and [3]. They consists of: (only one element of each class or family is given).
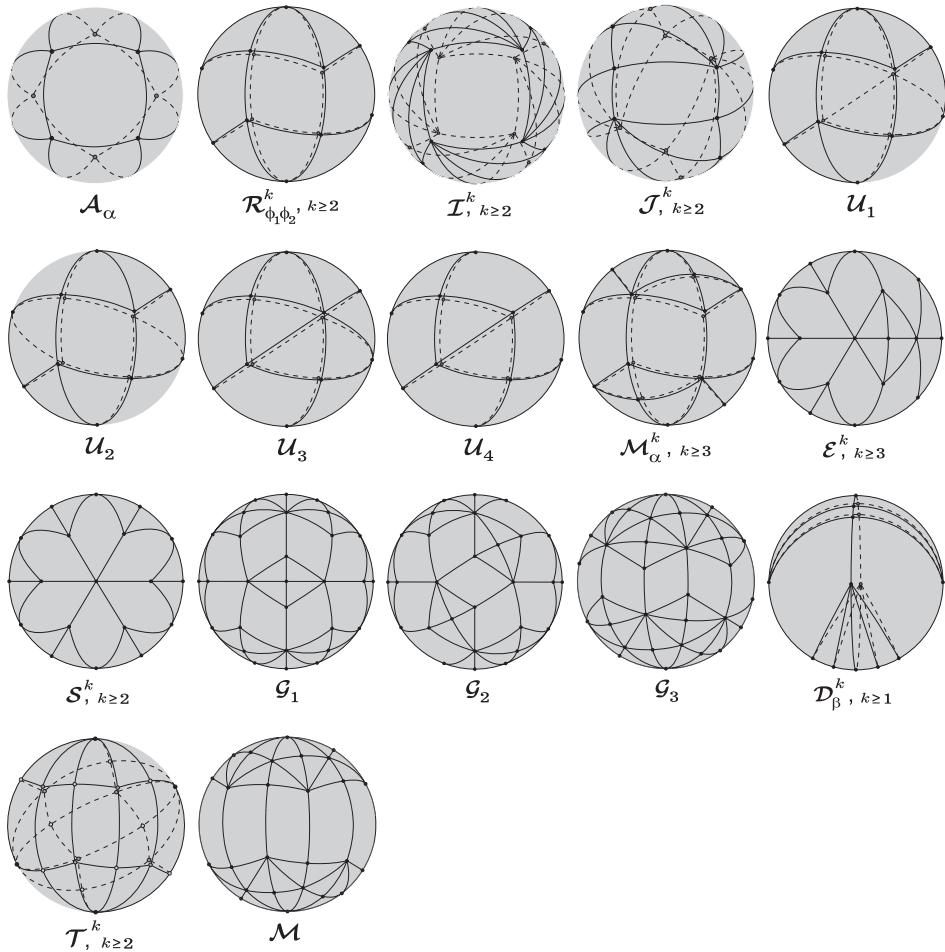
Fig. 80. Dihedral f-tilings of the sphere by triangles and WCSQ.

- *A family of square antiprisms* $(\mathscr{A}_\alpha)_{\alpha \in [\alpha_0, \pi[}$, in which T is an isosceles triangle iff $\alpha \in \{\alpha_0, \frac{2\pi}{3}\}$, where $\alpha_0 = \arccos(1 - \sqrt{2}) \approx 114.47°$ and α is internal angle of Q;

- For each $k \geq 2$ *a family of $2k$-polygonal radially elongated dipyramids,* $\mathscr{R}^k_{\phi_1 \phi_2}$;

- *A class of f-tilings* $\mathscr{I}^k$ $(k \geq 2)$, in which Q is a square and T is a scalene triangle. We illustrate $\mathscr{I}^2$.

- *A class of f-tilings* $\mathscr{J}^k$ $(k \geq 2)$. Q is a spherical quadrangle with all congruent angles and with distinct pairs of congruent opposite sides. T is a scalene triangle. We consider $k = 2$.

- *F-tilings $\mathscr{U}_i$, $i = 1, 2, 3, 4$, with the same prototiles. Q has all congruent sides and distinct pairs of angles. T is an isosceles triangle (note: there exists one another element of the form $\mathscr{R}^3_{\phi_1\phi_2}$ with such prototiles);*
- *For each $k \geq 3$ a family of f-tilings $\mathscr{M}^k_\alpha$ $\left(\frac{\pi}{k} < \alpha < \frac{2\pi}{k}\right)$, in which Q has distinct pairs of angles and T is a scalene triangle. In Figure we take the minimum value of k;*
- *Two classes of f-tilings $\mathscr{E}^k$ and $\mathscr{S}^{k-1}$ $(k \geq 3)$ such that Q has all congruent sides and distinct pairs of angles and T is a scalene triangle. We illustrate $\mathscr{E}^3$ and $\mathscr{S}^3$;*
- *F-tilings $\mathscr{G}_i$, $i = 1, 2, 3$, with the same prototiles. Q has all congruent sides and distinct pairs of angles. T is scalene;*
- *For each $k \geq 1$ a family of f-tilings $\mathscr{D}^k_\beta$ $\left(0 < \beta < \frac{\pi}{2k}\right)$ in which Q has distinct pairs of angles and distinct pairs of sides and T is isosceles. In Figure $\mathscr{D}^2_\beta$ is illustrated;*
- *A class of f-tilings $\mathscr{T}^k$ $(k \geq 2)$ in which Q has distinct pairs of angles and distinct pairs of sides and T is scalene. We illustrate $\mathscr{T}^2$;*
- *A f-tiling $\mathscr{M}$ such that Q has distinct pairs of angles and distinct pairs of sides and T is scalene.*

Acknowledgements

References

[1] A. M. d'Azevedo Breda and A. F. Santos, Well centered spherical quadrangles, Beiträge Algebra Geometrie, **44** (2003), 539–549.

[2] A. M. d'Azevedo Breda and A. F. Santos, Dihedral f-tilings of the sphere by spherical triangles and equiangular well-centered quadrangles, Beiträge Algebra Geometrie, **45** (2004), 441–461.

[3] A. M. d'Azevedo Breda and A. F. Santos, Dihedral f-tilings of the sphere by rhombi and triangles, Discrete Math. Theoretical Computer Sci., **7** (2005), 123–140.

[4] A. M. d'Azevedo Breda, A class of tilings of S^2, Geometriae Dedicata, **44** (1992), 241–253.

[5] H. L. Davies, Packings of spherical triangles and tetrahedra, in Proceedings of the Colloquium on Convexity (ed. W. Fenchel), Kobenhavns Univ. Mat. Inst., Copenhagen, 42–51, 1967.

[6] H. R. Farran, E. E. Kholy and S. A. Robertson, Folding a surface to a polygon, Geometriae Dedicata, **63** (1996), 255–266.

[7] J. Lawrence and J. E. Spingarn, An intrinsic characterization of foldings of euclidean space, Ann. Inst. H. Poincaré, Analyse Non Linéaire, **6** (1989), 365–383.

[8]　S. A. Robertson,　Isometric folding of riemannian manifolds,　Proc. Royal Soc. Edinb. Sect. A, **79** (1977), 275–284.

[9]　S. A. Robertson and E. E. Kholy,　Topological foldings,　Comm. Fac. Sci. Uni. Ankara, Ser. A1, **35** (1986), 101–107.

[10]　D. M. Y. Sommerville,　Division of space by congruent triangles and tetrahedra,　Proc. Royal Soc. Edinb., **43** (1992), 85–116.

[11]　Y. Ueno and Y. Agaoka,　Classification of tilings of the 2-dimensional sphere by congruent triangles,　Hiroshima Math. J., **32** (2002), 463–540.

[12]　Y. Ueno and Y. Agaoka,　Examples of spherical tilings by congruent quadrangles,　Mem. Fac. Integrated Arts and Sci., Hiroshima Univ. Ser. IV **27** (2001), 135–144.

Ana M. d'Azevedo Breda
Department of Mathematics
University of Aveiro
3810-193 *Aveiro*
Portugal
E-mail: ambreda@mat.ua.pt

Altino F. Santos
Department of Mathematics
U.T.A.D.
5001-911 *Vila Real*
Portugal
E-mail: afolgado@utad.pt